

Contents

1. Biology.....	3
Small scale reactions.....	3
Scale up procedure.....	3
2. Chemistry.....	3
General remarks.....	3
Compounds characterization.....	4
(<i>S</i>)-(+)-4-hydroxy-3,4-dihydronaphthalen-1(<i>2H</i>)-one (2a).....	4
(<i>R</i>)-(-)-4-hydroxy-6-methoxy-3,4-dihydronaphthalen-1(<i>2H</i>)-one (2b).....	4
(<i>S</i>)-(+)-4-hydroxy-7-methoxy-3,4-dihydronaphthalen-1(<i>2H</i>)-one (2c).....	4
(<i>S</i>)-(+)-3-hydroxy-2,3-dihydro-1 <i>H</i> -inden-1-one (4).....	5
(<i>S</i>)-(+)-2,3-dihydro-1 <i>H</i> -inden-1-ol (6a).....	5
(<i>S</i>)-(+)-1,2,3,4-tetrahydronaphthalen-1-ol (6b).....	5
Table S1. Previously evolved P450-BM3 mutants tested in the present study.....	6
Absolute configuration determination.....	7
General Mosher reaction.....	7
Compound S1.....	7
Compound S2.....	8
3. Molecular docking calculations.....	9
Molecular dynamics simulation details.....	10
Molecular dynamics simulations results.....	11
4. Selected NMR spectra.....	17
¹ H NMR (300 MHz, CDCl ₃) and ¹³ C NMR (75 MHz, CDCl ₃) spectra of 2a.....	17
¹ H NMR (300 MHz, CDCl ₃) and ¹³ C NMR (75 MHz, CDCl ₃) spectra of 2b.....	18
¹ H NMR (300 MHz, CDCl ₃) and ¹³ C NMR (75 MHz, CDCl ₃) spectra of 2c.....	19
¹ H NMR (300 MHz, CDCl ₃) and ¹³ C NMR (75 MHz, CDCl ₃) spectra of 4.....	20
¹ H NMR (300 MHz, CDCl ₃) and ¹³ C NMR (75 MHz, CDCl ₃) spectra of 6a.....	21
¹ H NMR (300 MHz, CDCl ₃) and ¹³ C NMR (75 MHz, CDCl ₃) spectra of 6b.....	22
5. Selected GC chromatograms.....	23
Reaction product (2a) resulting from α-tetralone (1a) biohydroxylation reaction with WT-P450.....	23
Reaction product (2a) resulting from α-tetralone (1a) biohydroxylation reaction with A328F-P450.....	23
Reaction product (2b) resulting from 6-methoxy-3,4-dihydronaphthalen-1(<i>2H</i>)-one (1b) biohydroxylation reaction with WT-P450.....	24
Reaction product (2c) resulting from 7-methoxy-3,4-dihydronaphthalen-1(<i>2H</i>)-one (1c) biohydroxylation reaction with WT-P450.....	25

Reaction product (4) resulting from 2,3-dihydro-1 <i>H</i> -inden-1-one (3) biohydroxylation reaction with WT-P450.....	26
Reaction product (4) resulting from 2,3-dihydro-1 <i>H</i> -inden-1-one (3) biohydroxylation reaction with A328R-P450	26
Reaction product (6a) resulting from 2,3-dihydro-1 <i>H</i> -indene (5a) biohydroxylation reaction with WT-P450.....	27
Reaction product (6a) resulting from 2,3-dihydro-1 <i>H</i> -indene (5a) biohydroxylation reaction with A328F-P450.....	27
Reaction product (6b) resulting from 1,2,3,4-tetrahydrodecaline (5b) biohydroxylation reaction with WT-P450.....	28
Reaction product (6b) resulting from 1,2,3,4-tetrahydrodecaline (5b) biohydroxylation reaction with A328F-P450.....	28

1. Biology

Reagents, experimental procedures, library A328 (NNK) creation and GC-based screening were previously described.^[1] *E. coli* BOU730 [an *E. coli* strain derived from *E. coli* BL21(DE3) that contains inserted into its genome a copy of the *gdh* gene from *B. megaterium* under the control of the T7 promoter]^[1a] was used in all biotransformations. Protein concentration, reaction conversions and TOF numbers were calculated as previously described.^[1c] A comprehensive list of previously evolved P450 mutants tested in this study is shown in **Table S1**.

Small scale reactions

Small scale reactions performed with P450-BM3 were carried out following our standard protocols. Briefly: 1 mL frozen pellets of BOU730 cells overexpressing desired WT or mutant P450-BM3 produced as describe previously,¹ were thawed and resuspended in 500 μ L of lysis buffer [phosphate buffer (pH 7.4, 100 mM), lysozyme (14 mg/mL), DNase I (6 U/mL)]. Samples were incubated at 37°C for 45 min and then centrifuged 15 min at 10000 r.p.m. The supernatant (445 μ L) was transferred to a new 1.5 mL tube containing 50 μ L of glucose (100 mM final concentration), 5 μ L of NADP⁺ (250 μ M final concentration) and 5 mM of the corresponding starting material **1a-c**, **3** or **5a-b**. Reactions were incubated for 20 hours at 25°C, extracted with ethyl acetate (500 μ L) and the organic phase subjected to GC analysis.

Scale up procedure

Scaling up reactions using P450-BM3 mutants and starting materials **1a-c**, **3** and **5a-b** were performed using the same protocol: a single colony of BOU730 cells containing the mutant of interest grown on lysogeny broth (LB) agar plates containing kanamycin (kan; 50 μ g/mL), was inoculated in LB medium (20 mL) with kan (50 μ g/mL) and incubated at 37°C. After 5 hours, this preinoculum was added to terrific broth (TB) medium (400 mL) containing kan (50 μ g/mL). The culture was incubated at 30°C until an O.D. of 0.8-0.9 at 600 nm was reached. Then, isopropyl β -D-1-thiogalactopyranoside (IPTG, 0.2 mM) was added in the culture for P450-BM3 overexpression, and the culture stirred at 30°C overnight. Cells were pelleted by centrifugation (15 min, 4000 r.p.m. at 4°C), the supernatant discarded and the pellet resuspended in 60 mL reaction buffer (phosphate buffer pH 7.4, 100 mM, glucose 100 mM, and NADP⁺ 200 μ M). The biohydroxylation reaction was started with the addition of the proper starting material and was left to react for 15-18 h for **1a-c**, **3** and 2 hours for **5a-b** at 25°C with mild agitation. After this time, the reaction mixture was extracted with ethyl acetate and the reaction crude was purified by column chromatography.

2. Chemistry

General remarks

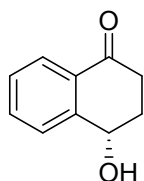
Starting materials were purchased from Sigma-Aldrich, Acros and TCI, and were used without further purification. NMR spectra were recorded on a Bruker Avance 300 (¹H: 300 MHz, ¹³C: 75 MHz) spectrometer using TMS as internal standard (d=0). High resolution EI mass spectra were measured on a Finnigan MAT 95S spectrometer. Conversion and enantiomeric excess were determined by achiral and chiral gas chromatography, as described. Optical rotation measurements were performed on a Rudolph Research Analytical Autopol IV at 25°C.

¹ a) R. Agudo, G.-D. Roiban, M. T. Reetz, *ChemBioChem*, **2012**, *13*, 1465-1473; b) G.-D. Roiban, R. Agudo, M. T. Reetz, *Tetrahedron* **2013**, *69*, 5306-5311; c) G.-D. Roiban, R. Agudo, M. T. Reetz, *Angew. Chem. Int. Ed.* **2014**, DOI: 10.1002/anie.201310892.

Compounds characterization

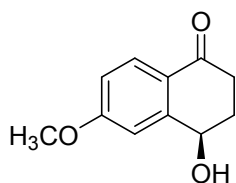
Compounds underwent reaction according to the general scale up procedure and were then purified by column chromatography.

(*S*)-(+)-4-hydroxy-3,4-dihydronaphthalen-1(2*H*)-one (**2a**)



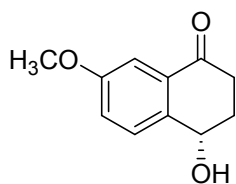
The absolute configuration of (*S*)-**2a** was assigned by comparison with an authentic sample, as reported by Kündig et al.^[2] Appearance: Viscous oil; ¹H NMR (300 MHz, CDCl₃) δ 7.97 (d, ³J = 7.7 Hz, 1H), 7.65–7.51 (m, 2H), 7.41–7.36 (m, 1H), 4.97–4.93 (m, 1H), 2.94–2.85 (m, 1H), 2.70 (s, 1H, OH), 2.61–2.51 (m, 1H), 2.42–2.32 (m, 1H), 2.21–2.13 (m, 1H). ¹³C NMR (75 MHz, CDCl₃) δ 197.8, 145.5, 134.2, 131.2, 128.3, 127.1 (2C), 67.8, 35.2, 32.1. HRMS (EI) calcd for C₁₀H₁₀O₂ [*M*]⁺: 162.0681; found: 162.0677.

(*R*)-(-)-4-hydroxy-6-methoxy-3,4-dihydronaphthalen-1(2*H*)-one (**2b**)



The absolute configuration of (*R*)-**2b** was assigned by comparing the optical rotation sign with (*S*)-**2a**. Also, a racemic mixture of the alcohol, and an enantiomeric pure alcohol, were respectively derivatized with Mosher chloride ((*R*)-(-)- α -methoxy- α -(trifluoromethyl)phenylacetyl chloride). The NMR spectra of the enantiomerically pure alcohol **2b** showed the (*R*)-configuration (see NMR spectra bellow). In addition, molecular docking calculations confirmed also the (*R*)-configuration. Appearance: Viscous oil; ¹H NMR (300 MHz, CDCl₃) δ 8.00 (d, ³J = 8.7 Hz, 1H), 7.10 (d, ³J = 2.1 Hz, 1H), 6.91 (dd, ³J = 8.7, 2.6 Hz, 1H), 4.95–4.91 (m, 1H), 3.89 (s, 3H), 2.91–2.82 (m, 1H), 2.62–2.52 (m, 1H), 2.44–2.37 (m, 1H), 2.20–2.14 (m, 1H). ¹³C NMR (75 MHz, CDCl₃) δ 196.1, 164.4, 148.1, 129.9, 124.8, 114.7, 110.9, 68.4, 55.7, 35.3, 32.6. HRMS (EI) calcd for C₁₁H₁₂O₃ [*M*]⁺: 192.0786; found: 192.0788.

(*S*)-(+)-4-hydroxy-7-methoxy-3,4-dihydronaphthalen-1(2*H*)-one (**2c**)

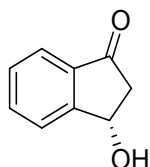


The absolute configuration of (*S*)-**2c** was assigned by comparing the optical rotation sign with (*S*)-**2a**. Also, a racemic mixture of the alcohol, and an enantiomeric pure alcohol, were respectively

² A. E. Garcia, S. Ouizem, X. Cheng, P. Romanens, E. P. Kundig, *Adv. Synth. Catal.* **2010**, 352, 2306-2314.

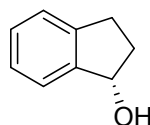
derivatized with Mosher chloride ((*R*)-(-)- α -methoxy- α -(trifluoromethyl)phenylacetyl chloride). The NMR spectra of the enantiomerically pure alcohol **2c** showed the (*S*)-configuration (see NMR spectra below). Appearance: Viscous oil which crystallizes in the fridge. ^1H NMR (300 MHz, CDCl_3) δ 7.50–7.48 (m, 2H), 7.15 (dd, $J = 8.5, 2.8$ Hz, 1H), 4.95 (dd, $J = 7.3, 3.8$ Hz, 1H), 3.85 (s, 3H), 3.00–2.89 (m, 1H), 2.64–2.54 (m, 1H), 2.43–2.33 (m, 1H), 2.25–2.11 (m, 1H). ^{13}C NMR (75 MHz, CDCl_3) δ 197.5, 159.8, 138.0, 132.4, 128.9, 122.0, 109.5, 67.5, 55.7, 34.9, 32.2. HRMS (EI) calcd for $\text{C}_{11}\text{H}_{12}\text{O}_3$ [M] $^+$: 192.0786; found: 192.0784.

(*S*)-(+)-3-hydroxy-2,3-dihydro-1*H*-inden-1-one (**4**)



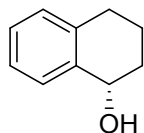
The absolute configuration of (*S*)-**4** was assigned by comparison with an authentic sample, as reported by Nair et al.^[3] Appearance: pale yellow oil. ^1H NMR (300 MHz, CDCl_3) δ 7.73–7.64 (m, 3H), 7.49–7.44 (m, 1H), 5.42 (dd, $J = 6.8, 2.9$ Hz, 1H), 3.10 (dd + br s (OH), $J = 18.9$ Hz, 6.0 Hz, 2H), 2.61 (dd, $J = 18.9$ Hz, 3.0 Hz, 1H). ^{13}C NMR (75 MHz, CDCl_3) δ 203.5, 155.3, 136.5, 135.4, 129.6, 126.0, 123.3, 68.6, 47.3. HRMS (EI) calcd for $\text{C}_9\text{H}_8\text{O}_2$ [M] $^+$: 148.0524; found: 148.0518.

(*S*)-(+)-2,3-dihydro-1*H*-inden-1-ol (**6a**)



The absolute configuration of (*S*)-**6a** was assigned by comparison with an authentic sample, as reported by O'Brien et al.^[4] Appearance: cream powder. ^1H NMR (300 MHz, CDCl_3) δ 7.41–7.38 (m, 1H), 7.27–7.23 (m, 3H), 5.21–5.17 (m, 1H), 3.08–2.98 (m, 1H), 2.85–2.74 (m, 1H), 2.58 (br s, 1H, OH), 2.49–2.38 (m, 1H), 1.96–1.85 (m, 1H). ^{13}C NMR (75 MHz, CDCl_3) δ 145.0, 143.3, 128.2, 126.6, 124.8, 124.3, 76.3, 35.8, 29.8. HRMS (EI) calcd for $\text{C}_9\text{H}_{10}\text{O}$ [M] $^+$: 134.0732; found: 134.0735.

(*S*)-(+)-1,2,3,4-tetrahydronaphthalen-1-ol (**6b**)



The absolute configuration of (*S*)-**6b** was assigned by comparison with an authentic sample, as reported by Santoro et al.^[5] Appearance: Viscous oil; ^1H NMR (300 MHz, CDCl_3) δ 7.45–7.42 (m, 1H), 7.24–7.17 (m, 2H), 7.13–7.11 (m, 1H), 4.79 (t, $^3J = 4.7$ Hz, 1H), 2.88–2.67 (m, 2H), 2.02–1.78

³ S. Joly, M. S. Nair, *Tetrahedron: Asymmetry* **2001**, *12*, 2283-2287.

⁴ M. J. Dearden, C. R. Firkin, J. P. R. Hermet, P. O'Brien *J. Am. Chem. Soc.* **2002**, *124*, 11870-11871.

⁵ R. Patchett, I. Magpantay, L. Saudan, C. Schotes, A. Mezzetti, F. Santoro, *Angew. Chem. Int. Ed.* **2013**, *52*, 10352-10355.

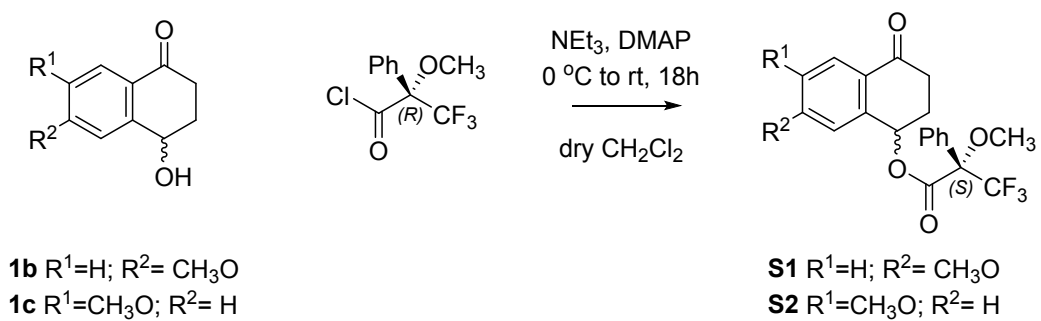
(m, 4H); ^{13}C NMR (75 MHz, CDCl_3) δ 138.9, 137.2, 129.1, 128.7, 127.7, 126.3, 68.3, 32.4, 29.3, 23.9, 18.9. HRMS (EI) calcd for $\text{C}_{10}\text{H}_{12}\text{O}$ [M] $^+$: 148.0888; found: 148.0889.

Table S1. Previously evolved P450-BM3 mutants tested in the present study

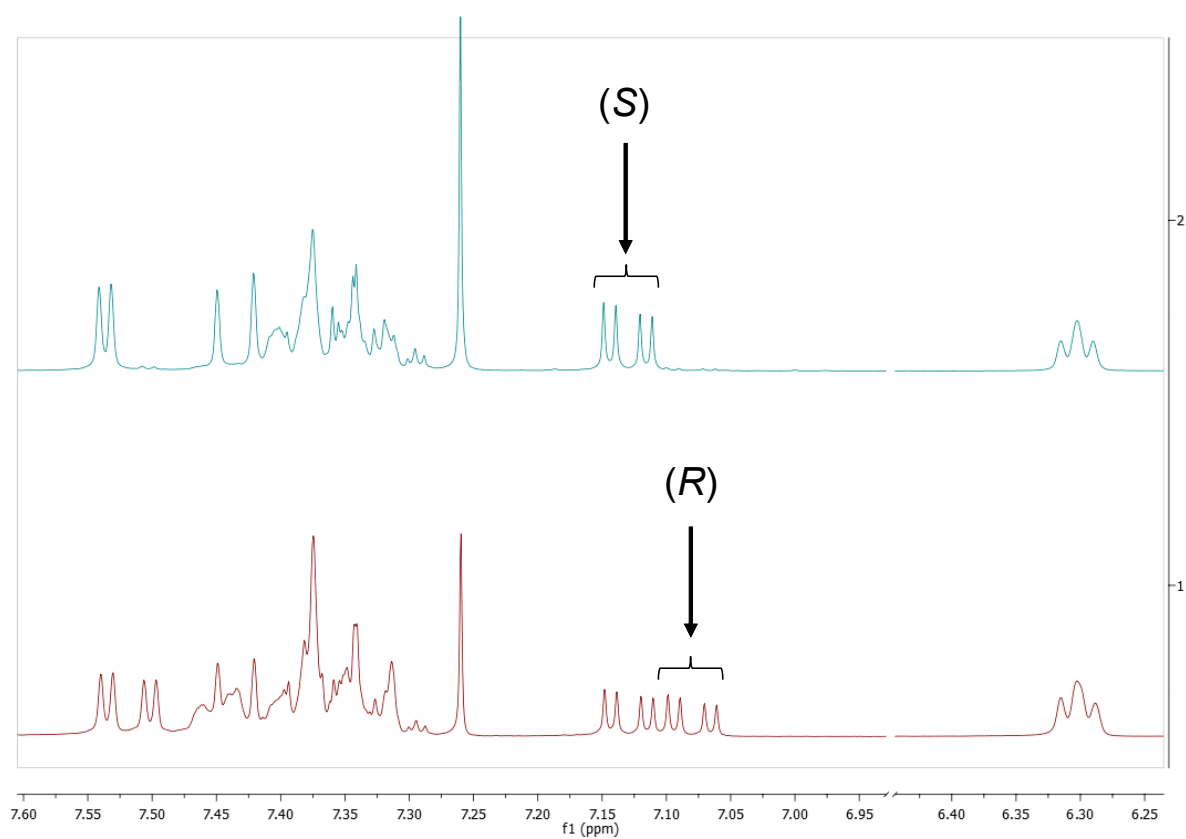
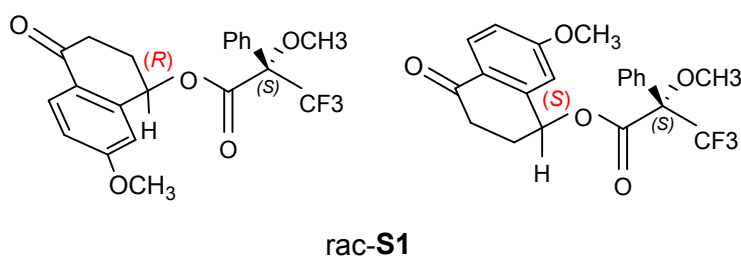
Mutant
V78F/L181F
V78F/L181H
V78H/L181F
V78W/L181F
V78W/L181R
V78K
V78W
L181F
L181K
F87A
F87G
F87L
F87R
F87S
F87T
F87V
T88S
T268K/A328W
T268K
A328F
A328H
A328K
A328R
A328W
A328Y

Absolute configuration determination

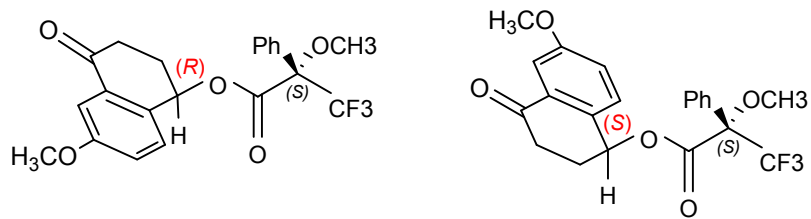
General Mosher reaction



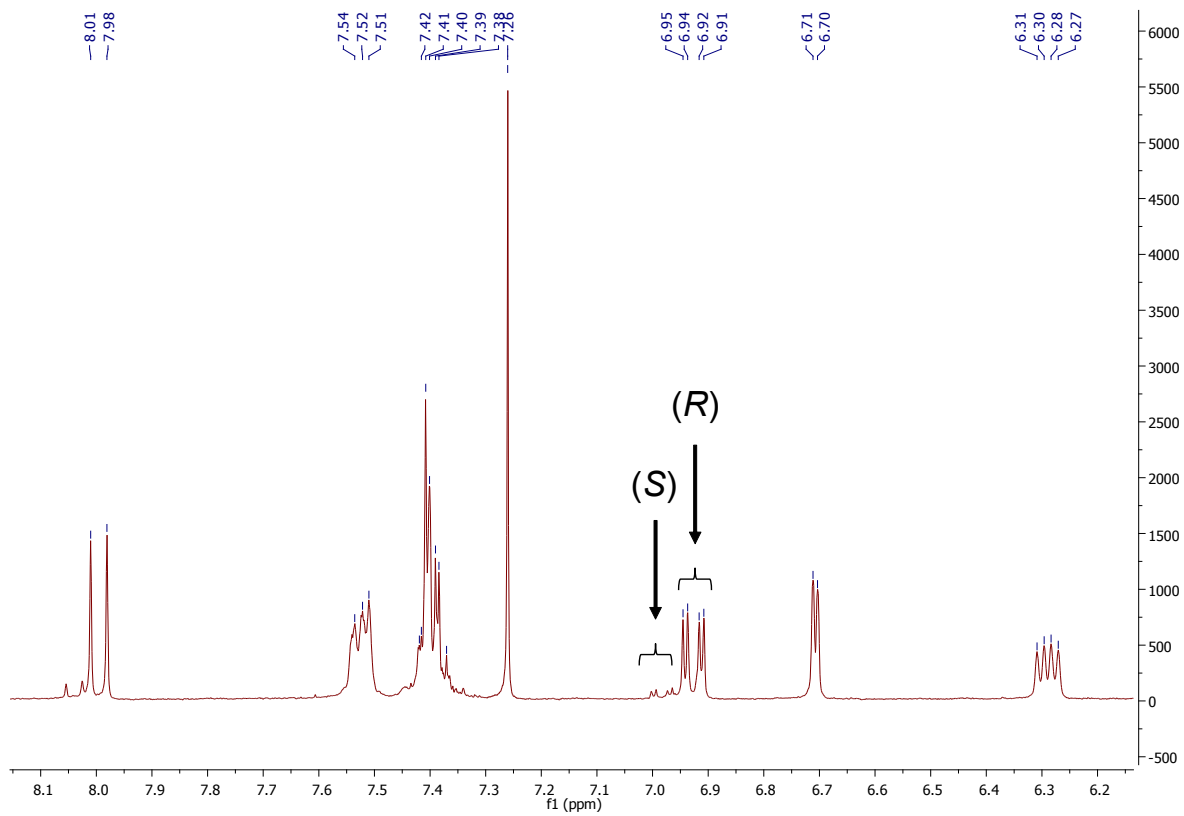
Compound S1



Compound S2



rac-S2



3. Molecular docking calculations

The structures of substrates **1a**, **1b** and **1c** were built in the Maestro program^[6] and a geometry optimization was performed at the BP86/SV level using ORCA (version 3.0.1).^[7] Docking calculations were performed using the Autodock Vina program,^[8] using the crystal structure of P450-BM3 complexed with N-palmitoylglycine^[9] (PDB entry 1JPZ). N-palmitoylglycine and the crystallographic water molecules were removed from the structure prior to the docking calculation. The coordinates of the missing residues (227-228) were obtained by superposition with the 1BU7 crystal structure.^[10] The protein was treated as a rigid receptor molecule. The search space used by the docking program was a 30 Å cube centered on the heme Fe. 30 docking poses were requested for each substrate.

For substrate **1a**, 18 docking poses were found, and 10 of these positioned the substrate in the active site. The 4th docking pose was selected, as this pose placed the substrate closest to the heme, in a position favoring the formation of the observed product (Figure 1).

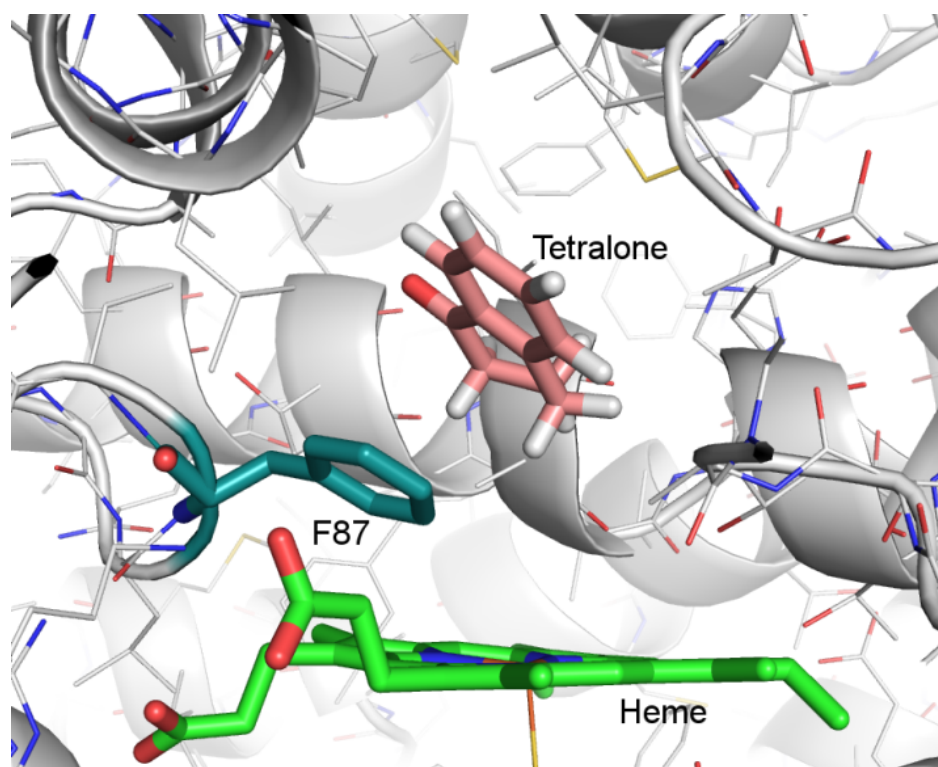


Figure 1 Docking pose 4 for substrate **1a** in WT P450-BM3. This structure was selected as the starting point for MD simulations

For the docking of substrate **1b**, 17 docking poses were found, with 8 of these placing the substrate in the active site. Only two of these poses placed one of the substrate hydrogen atoms within 6 Å of the heme iron. Out of these, the docking pose with the highest binding affinity (depicted in Figure 2), places the substrate in a position where the pro-*R* hydrogen is closest to the heme iron.

⁶ Maestro v9.6, 2013, Schrödinger LLC.

⁷ F. Neese, *Wiley Interdiscip. Rev.: Comput. Mol. Sci.* **2012**, *2*, 73–78.

⁸ O. Trott, A. J. Olson, *J. Comp. Chem.* **2010**, *31*, 455-461.

⁹ D. C. Haines, D. R. Tomchick, M. Machius, J. A. Peterson, *Biochemistry* **2001**, *40*, 13456-13465.

¹⁰ I. F. Sevioukova, H. Li, H. Zhang, J. A. Peterson, T. L. Poulos, *Proc. Natl. Acad. Sci. USA* **1999**, *96*, 1863-1868.

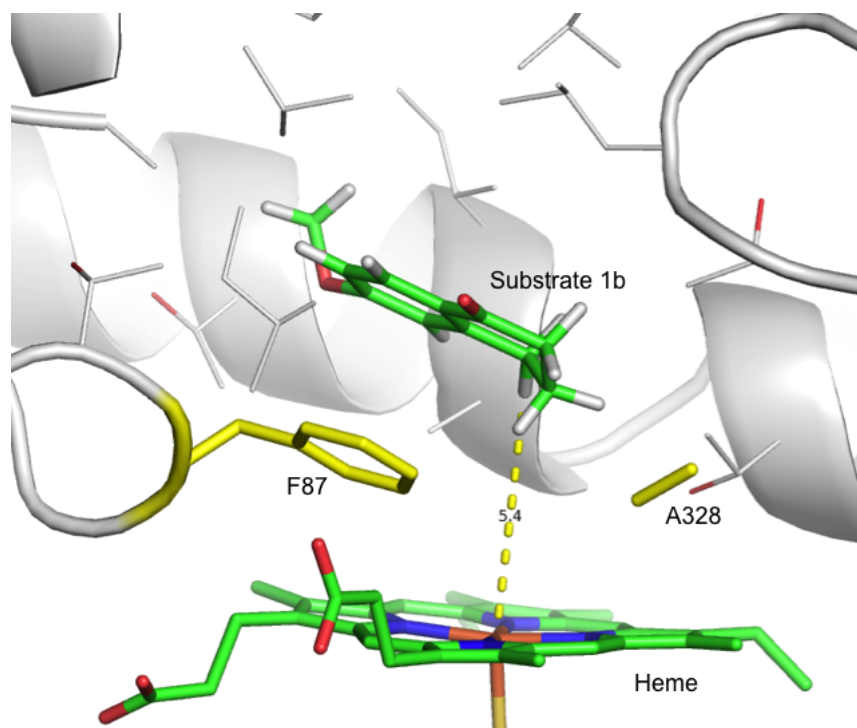


Figure 2 Docking pose 1 for substrate 1b in WT P450-BM3.

For the docking of substrate **1c**, 18 docking poses were found, with 11 of these placing the substrate in the active site cavity. Two docking poses (3 and 4) were placed the substrate within a reactive proximity of the heme, and these were found to have equal binding affinity (-7.0 kcal/mol). Docking poses 3 and 4 are displayed in Figure 3, and favor the formation of *R*-4-hydroxy-1-tetralone and *S*-4-hydroxy-1-tetralone, respectively.

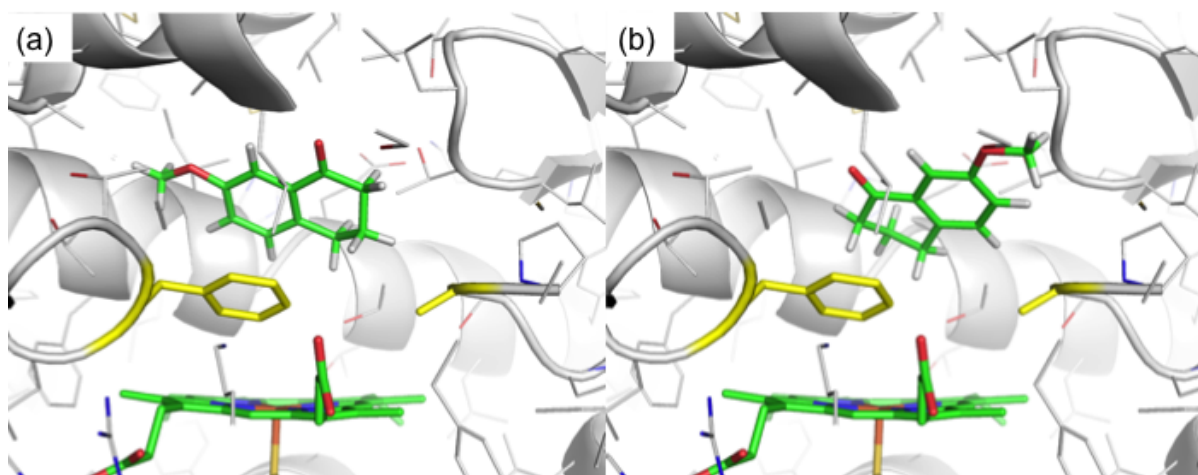


Figure 3. Docking poses (a) 3 and (b) 4 for substrate 1c in WT P450-BM3.

Molecular dynamics simulation details

Molecular dynamics simulations were performed on WT P450-BM3 (in the Compound I state), complexed with substrate **1a**, using the AMBER14 program.^[11] The initial structure was obtained from the docking calculation performed above. Hydrogen atoms were added using the *tleap* program.

¹¹ D. A. Case, V. Babin, J. T. Berryman, R. M. Betz, Q. Cai, D. S. Cerutti, T. E. Cheatham, III, T. A. Darden, R. E. Duke, H. Gohlke, A. W. Goetz, S. Gusarov, N. Homeyer, P. Janowski, J. Kaus, I. Kolossváry, A. Kovalenko, T. S. Lee, S. LeGrand, T. Luchko, R. Luo, B. Madej, K. M. Merz, F. Paesani, D. R. Roe, A. Roitberg, C. Sagui, R. Salomon-Ferrer, G. Seabra, C. L. Simmerling, W. Smith, J. Swails, R. C. Walker, J. Wang, R. M. Wolf, X. Wu and P. A. Kollman (2014), AMBER 14, University of California, San Francisco.

Protonation states of titratable amino acids were determined using the H++ server^[12] and visual inspection. The overall charge of the system ($-13e^-$) was neutralized by the addition of 13 Na^+ ions. The enzyme:substrate complex was solvated in a truncated octahedral box of 16050 explicit water molecules, simulated with the TIP3P water model.^[13] The water molecules contained in the 1JPZ crystal structure were retained in the model. The protein was treated with the FF14SB force field.^[14] MM parameters for the heme in the Compound I state were taken from reference^[15] and the parameters for tetralone were generated using the Generalized Amber ForceField (GAFF)^[16] using the ANTECHAMBER module of AmberTools13.^[11] The positions of all hydrogen atoms were firstly energy minimized using *sander*, with 200 steps of steepest descent (SD), followed by 1300 steps of conjugate gradient (CG) minimization. This procedure was then repeated for all atoms in the system. A cut-off of 15 Å was used for the calculation of non-bonded interactions during minimization. The system was next heated from 0 to 310 K over 50 ps of molecular dynamics using a time step of 2 fs in an NVT ensemble, with a harmonic restraint of force constant 4 kcal mol⁻¹ Å⁻² on all backbone heavy atoms. The restraint was then removed gradually (by 1 kcal mol⁻¹ Å⁻² each 250 ps) over 1 ns of MD equilibration using an NPT ensemble. During equilibration, a cut-off of 8 Å was used for non-bonded interactions, this was extended to 10 Å during the production phase MD. Two production phase NPT MD simulations of 48 ns were performed using the GPU implementation of *pmemd*^[17] at 300 K starting from the equilibrated structure, using different sets of initial velocities determined from a random seed. Periodic boundary conditions were employed using the Particle Mesh Ewald method for the calculation of electrostatic interactions. All bonds to hydrogen atoms were constrained using the SHAKE algorithm. Langevin temperature scaling was employed with a collision frequency of 2 ps⁻¹. Pressure regulation was performed at 1 bar with isotropic position scaling and a pressure relaxation time of 5 ps. Geometries were stored at 10 ps intervals.

Molecular dynamics simulations results

The root mean square deviation of the backbone heavy atoms from their initial positions, during the two 48 ns production phase MD simulations, is displayed in Figure 3. Some initial relaxation of the structure occurs during the first 20 ns, hence only the latter portion of the simulation is used for analysis purposes.

Tetralone was found to populate two distinct conformations in the active site of P450 BM3. One of these, considered to be the reactive conformation, has at least one substrate atom close enough to the heme for hydroxylation to occur (less than 4 Angstroms from the ferryl oxygen – see Figure 4). The other conformation was considered to be unreactive, as all hydrogen atoms were at a distance greater than 5 Å from the heme oxygen. In the unreactive conformation, the carbonyl oxygen of tetralone points in the direction of the heme oxygen (see Figure 5).

¹² a) <http://biophysics.cs.vt.edu/H++>; b) R. Anandakrishnan, B. Aguilar, A.V. Onufriev, *Nucleic Acids Res.* **2012**, *40*, W537-541; c) J. Myers, G. Grothaus, S. Narayanan, A. Onufriev *Proteins* **2006**, *63*, 928-938; d) J. C. Gordon, J. B. Myers, T Folta, V Shoja, L. S. Heath, A. Onufriev *Nucleic Acids Res.* **2005**, *33*, W368-71.

¹³ W. L. Jorgensen, J. Chandrasekhar, J. D. Madura, R. W. Impey, M. L. Klein, *J. Chem. Phys.* **1983**, *79*, 926-935.

¹⁴ V. Hornak, R. Abel, A. Okur, B. Strockbine, A. Roitberg, *Proteins*, **2006**, *65*, 712-725.

¹⁵ K. Shahrokh, A. Orendt, G. S. Yost, T. E. Cheatham, *J. Comput. Chem.* **2012**, *33*, 119-133.

¹⁶ J. Wang, R. M. Wolf, J. W. Caldwell, P. A. Kollman, D. A. Case, *J. Comput. Chem.* **2004**, *25*, 1157-1174.

¹⁷ a) R. Salomon-Ferrer, A. W. Goetz, D. Poole, S. Le Grand, R. C. Walker, *J. Chem. Theory Comput.*, **2013**, *9*, 3878-3888; b) A. W. Goetz, M. J. Williamson, D. Xu, D. Poole, S. Le Grand, R. C. Walker, *J. Chem. Theory Comput.*, **2012**, *8*, 1542-1555; c) S. Le Grand, A. W. Goetz, R. C. Walker, *Comp. Phys. Comm.*, **2013**, *184*, 374-380.

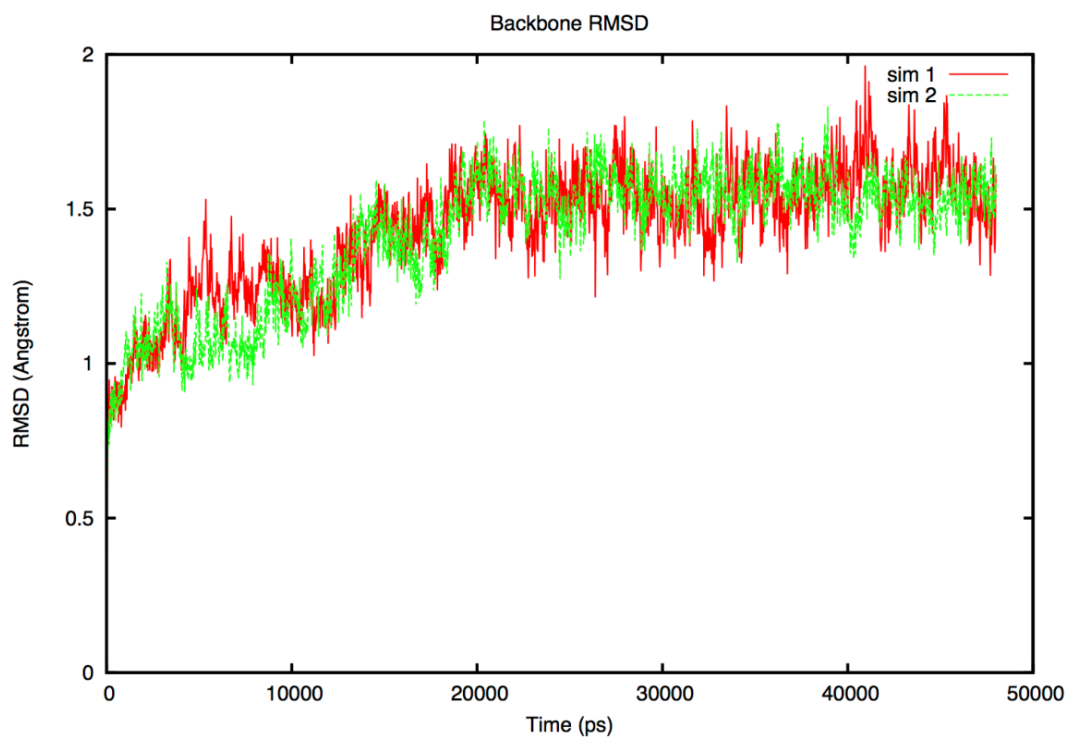


Figure 3 Root mean square deviation (RMSD) of the backbone heavy atoms during 2 x 48 ns molecular dynamics simulations of tetralone in P450BM3

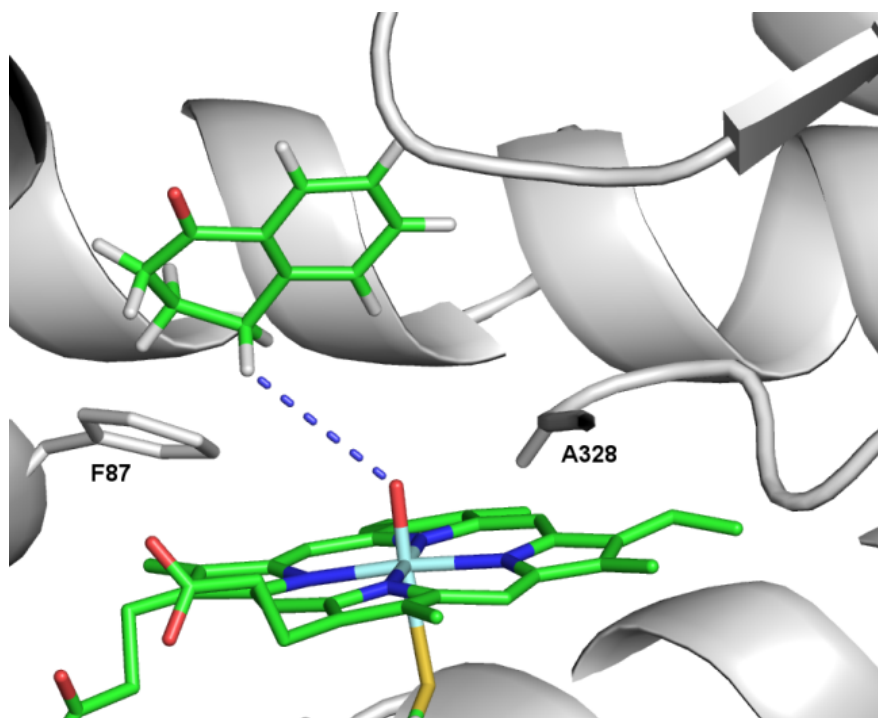


Figure 4 Structure obtained from simulation 2 after 34,940 ps. The O-H distance between the ferryl oxygen of Compound I and the pro-S hydrogen attached to C4 of tetralone is highlighted by the blue dashed line. The F87 and A328 residues are also highlighted in white stick form.

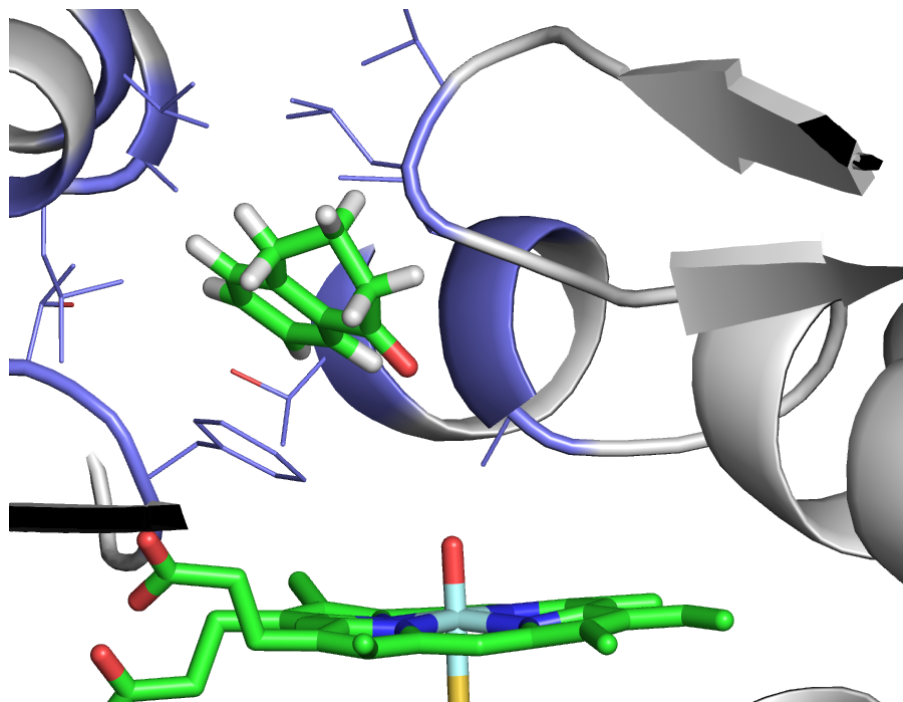


Figure 5 Unreactive binding pose of tetralone in P450-BM3 from molecular dynamics simulations. Structure obtained from simulation 1 after 48 ns.

During the equilibration phase (20 ns) of simulation 1, the substrate moves from the reactive to the unreactive binding conformation. The substrate remains in the unreactive conformation for the entirety of the production phase (as shown in Figure 5).

During simulation 2, both the reactive and unreactive binding conformations of the substrate are sampled. Movement between the two conformations is reversible. The distance between the Compound I oxygen atom and the two hydrogen atoms connected to C4 of tetralone (H4R and H4S) was monitored (see Figure 6), together with the Fe-O-H4RS angle (Figure 7).

The average distance between the ferryl oxygen of Compound I, and each of the hydrogen atoms attached to tetralone, calculated over each simulation, is displayed in Table 1. The closest hydrogen atom to the Compound I oxygen on average during simulation 1 is the one attached to C8, however, this carbon is an aromatic carbon. In previous QM^[18] and QM/MM^[19] studies of aromatic hydroxylation, it was found that this reaction proceeds via C-O bond formation between the aromatic carbon of the substrate and the ferryl oxygen of Compound I. The preferred substrate orientation for aromatic oxidation by Compound I involves approach of the aromatic carbon, not the hydrogen atom. If only the aliphatic carbon atoms are taken into account, the closest hydrogen atom to the active oxidizing species is the pro-*R* hydrogen attached to C2. This is not consistent with the experimentally observed preference for hydroxylation at C4, however, this average distance is considered too long for reaction to be feasible (6.446 Å), and the binding of tetralone in this simulation is considered unreactive. In the second simulation, the shortest average O-H distance corresponds to the 4 pro-*S* hydrogen, which is consistent with the experimentally observed selectivity.

¹⁸ a) S. P. de Visser, S. Shaik, *J. Am. Chem. Soc.*, **2003**, *125*, 7413-7424; b) C. M. Bathelt, L. Ridder, A. J. Mulholland, J. N. Harvey, *Org. Biomol. Chem.* **2004**, *2*, 2998-3005.

¹⁹ C. M. Bathelt, A. J. Mulholland, J. N. Harvey, *J. Phys. Chem. A* **2008**, *112*, 13149-13156.

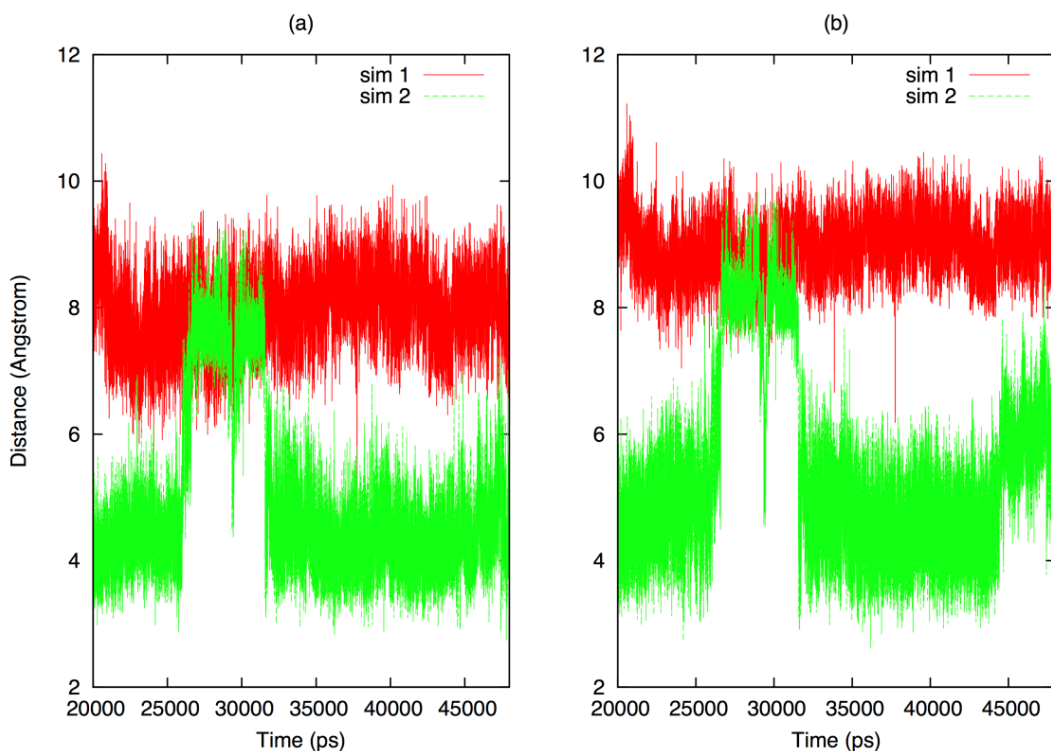


Figure 6 Distance between the ferryl oxygen of Compound I and the (a) *pro-S* and (b) *pro-R* hydrogen atoms connected to C4 of tetralone, calculated during 2 x 48 ns molecular dynamics simulations.

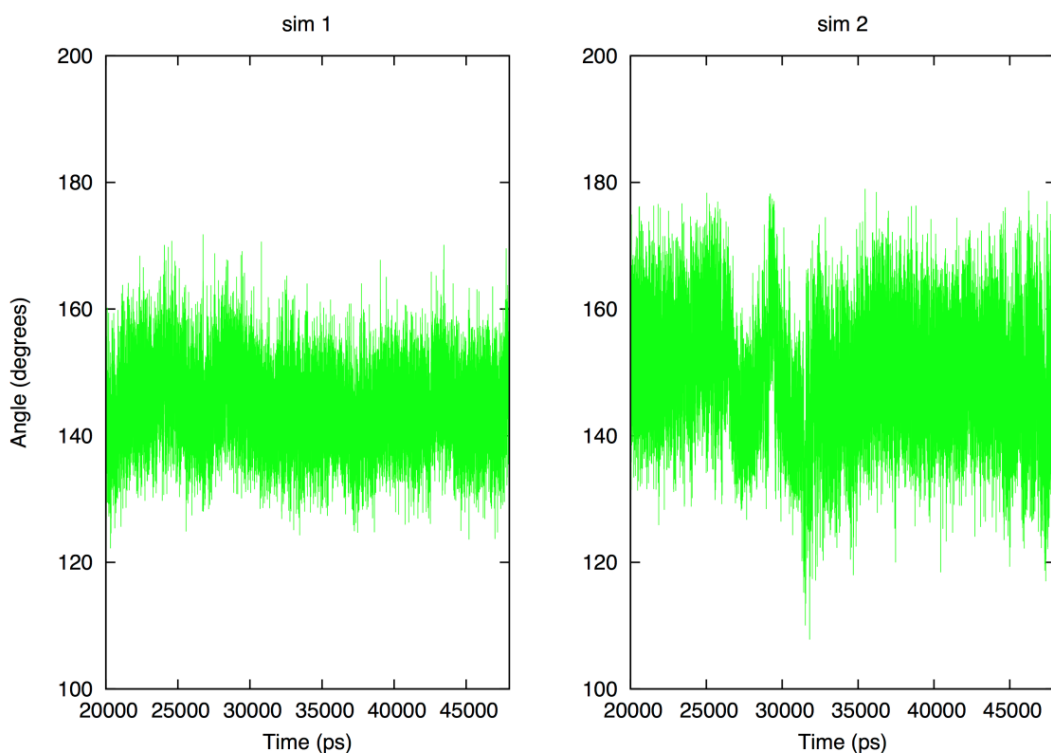


Figure 7 Angle between heme iron, ferryl oxygen and *pro-S* hydrogen atom connected to C4 (Fe-O-H) of tetralone, calculated during 2 x 48 ns molecular dynamics simulations

The populations of the observed O-H distances, calculated over the two MD simulations, are displayed in the form of a histogram in Figure 8. The peak corresponding to the shortest O-H distance is observed for the 4 *pro-S* hydrogen. An additional peak is observed for this distance at around 8 Å, and corresponds to the unreactive binding pose.

Out of the 28000 structures obtained during the production phase of simulation 2, 5782 had a O-H4S distance of shorter than 4 Å. Significantly fewer structures (3380) were found where the O-H4R distance was shorter than 4.0 Å, and in only 2293 of these structures was the O-H4R distance shorter than the O-H4S distance. It has been shown previously in QM^[20] and QM/MM^[21] studies of P450-catalyzed hydroxylation that the ideal angle of approach of the hydrogen atom to undergo hydroxylation is around 130 degrees. Hence, O-H4S reactive structures detailed above were further filtered based on the Fe-O-H4S angle. 111 structures were found where the Fe-O-H4S was between 110 and 140 degrees, representing only 0.4 % of the trajectory. An example structure satisfying these criteria is shown in Figure 4.

Table 1 Average distance between the ferryl oxygen atom of Compound I and the hydrogen atoms on the tetralone substrate molecule calculated over the last 28 ns of 2 x 48 ns molecular dynamics simulations. The experimentally observed major product is highlighted in bold. Standard deviations are provided in parentheses.

Hydrogen atom	Distance [Å]	
	Sim. 1	Sim. 2
2 pro- <i>R</i>	6.446 (0.954)	6.966 (0.897)
2 pro- <i>S</i>	6.768 (1.031)	7.893 (0.740)
3 pro- <i>R</i>	8.613 (0.821)	6.587 (1.259)
3 pro- <i>S</i>	8.236 (0.633)	7.011 (0.829)
4 pro- <i>R</i>	8.963 (0.451)	5.439 (1.470)
4 pro-<i>S</i>	7.952 (0.566)	4.968 (1.346)
5 (ar)	8.755 (0.556)	4.931 (1.201)
6 (ar)	8.155 (0.989)	6.112 (1.072)
7 (ar)	6.234 (1.170)	7.279 (1.895)
8 (ar)	4.707 (0.681)	7.625 (1.919)

²⁰ a) S. Shaik, D. Kumar, S. P. de Visser, A. Altun, W. Thiel, *Chem. Rev.* **2005**, *105*, 2279-2328; b) R. Lonsdale, J. N. Harvey, A. J. Mulholland, *J. Phys. Chem. Lett.* **2010**, *1*, 3232-3237.

²¹ R. Lonsdale, J. N. Harvey, A. J. Mulholland, *J. Phys. Chem. B* **2010**, *114*, 1156-1162.

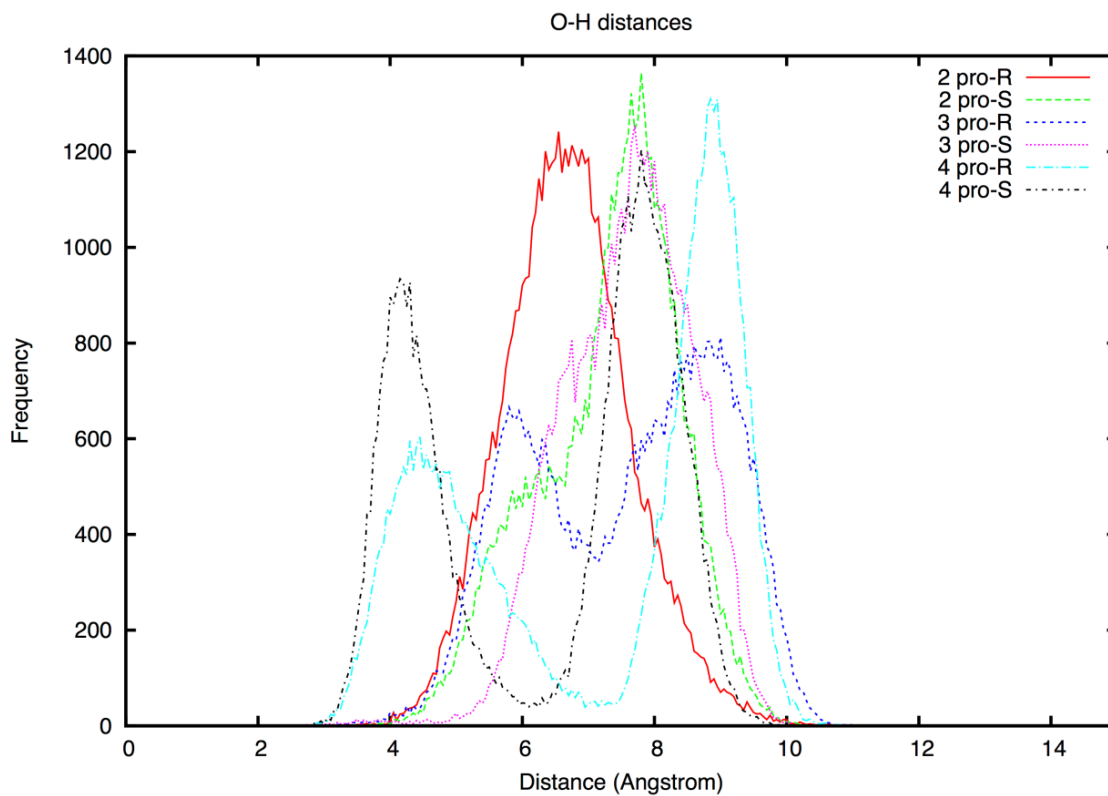
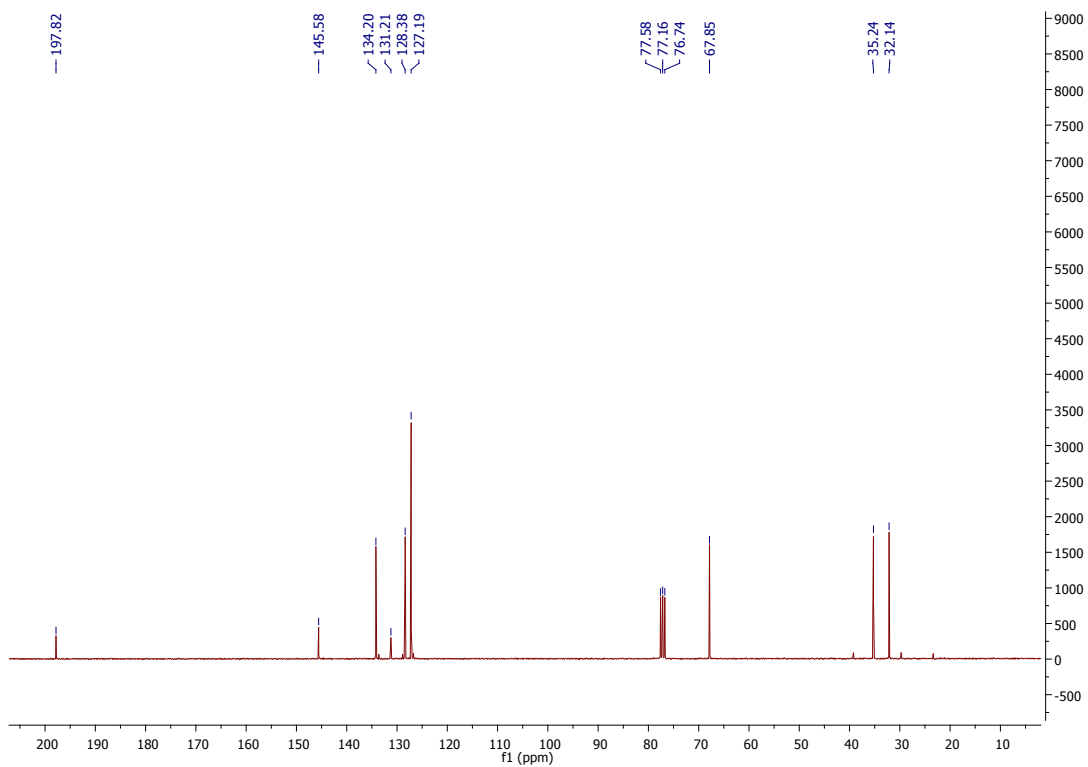
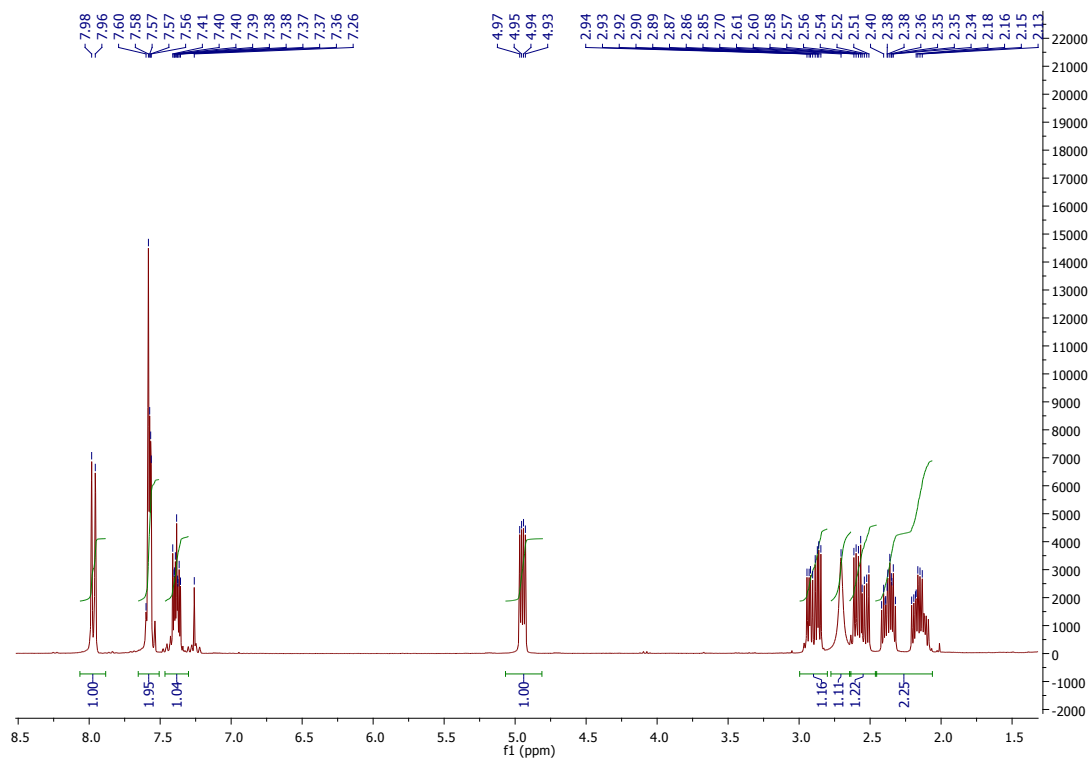
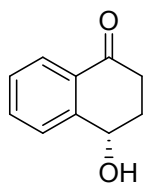


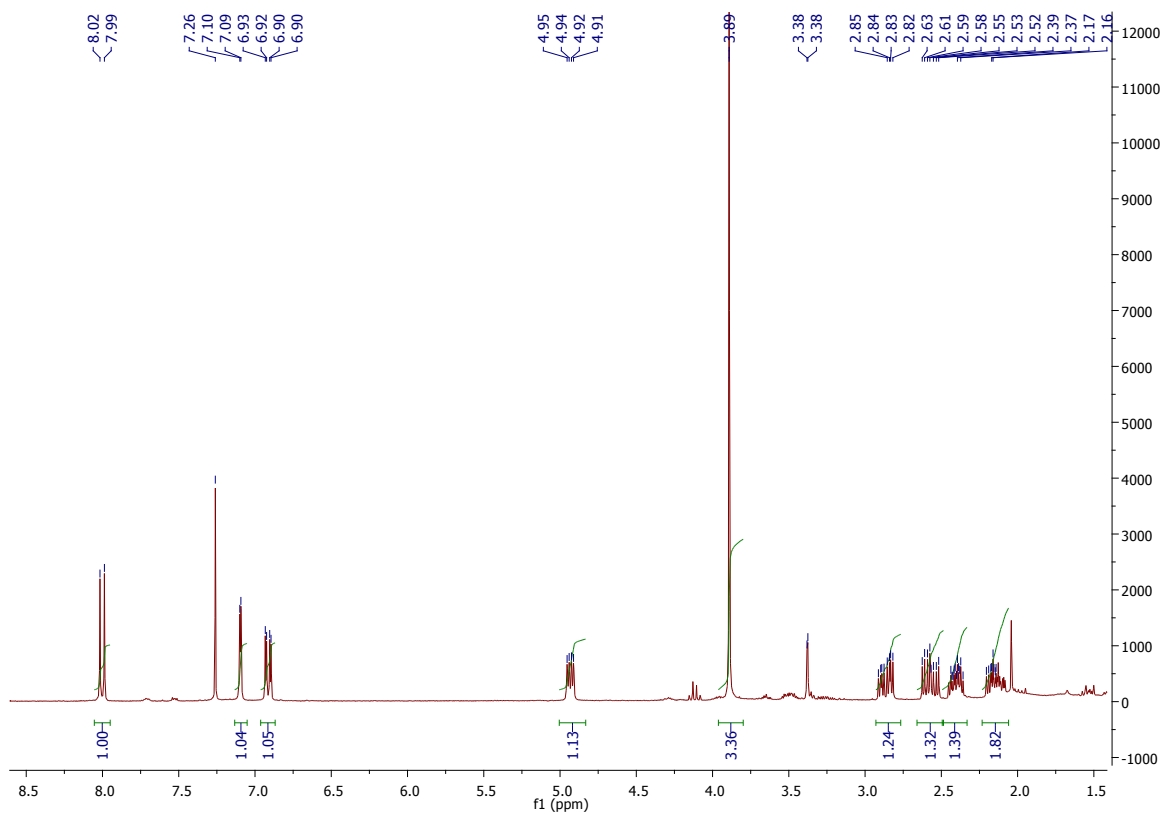
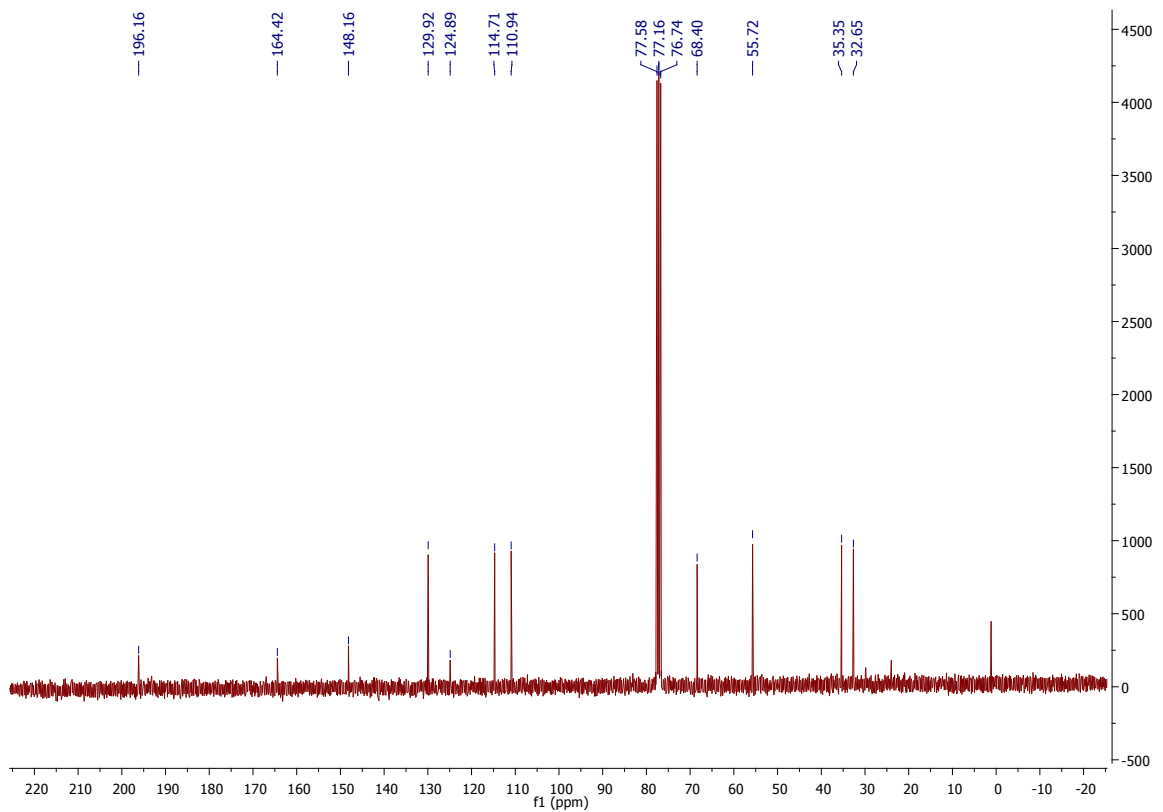
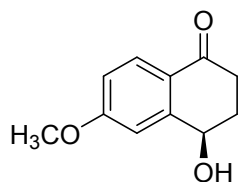
Figure 8 Histogram of distances between the aliphatic hydrogen atoms of tetralone and the ferryl oxygen of Compound I, calculated over 2 x 48 ns MD simulations

4. Selected NMR spectra

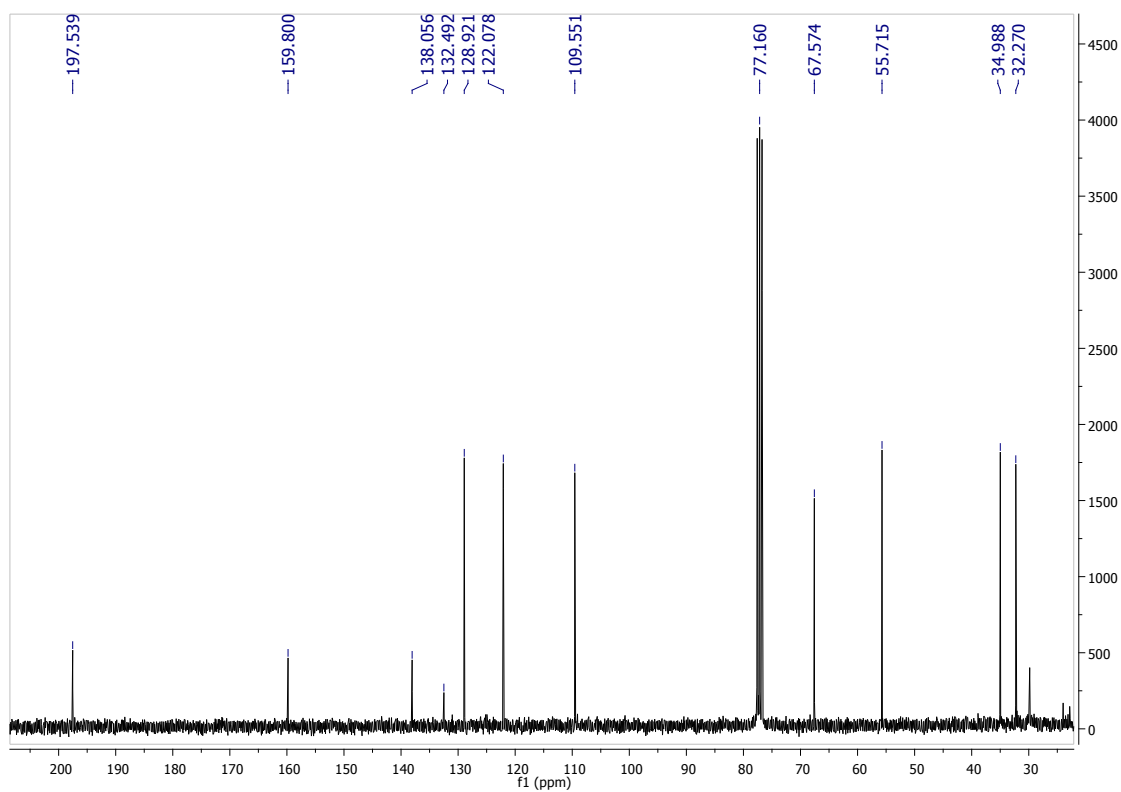
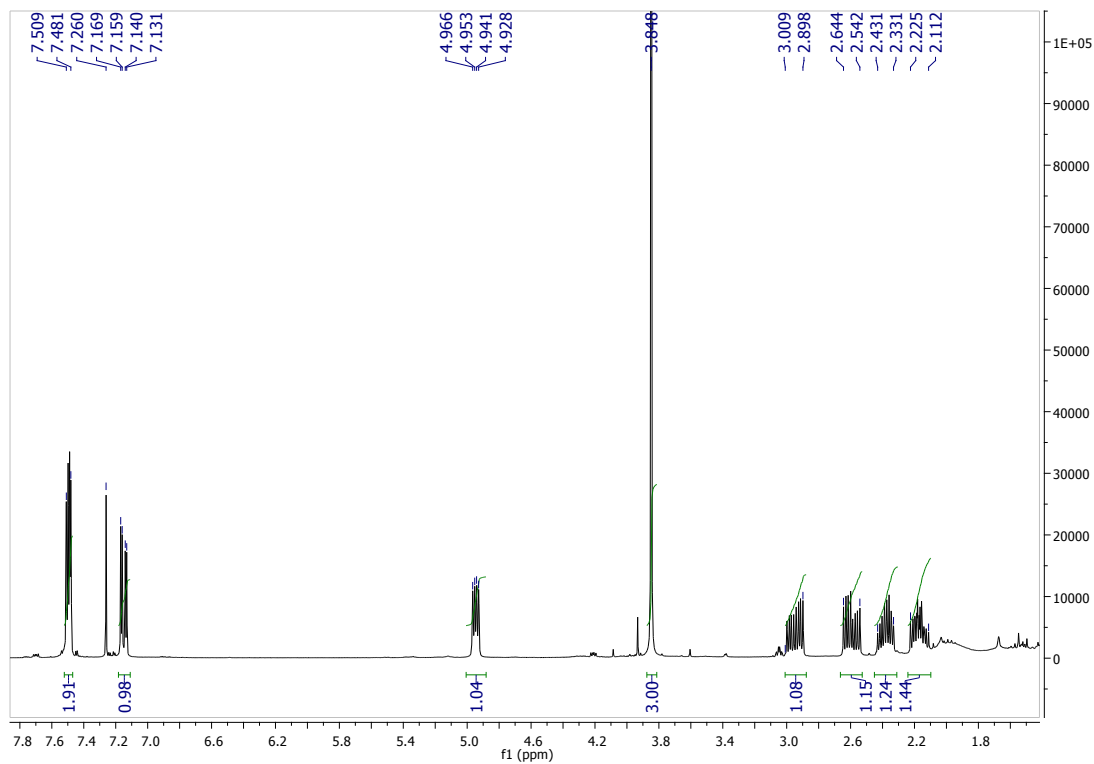
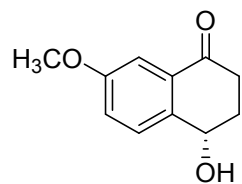
^1H NMR (300 MHz, CDCl_3) and ^{13}C NMR (75 MHz, CDCl_3) spectra of **2a**



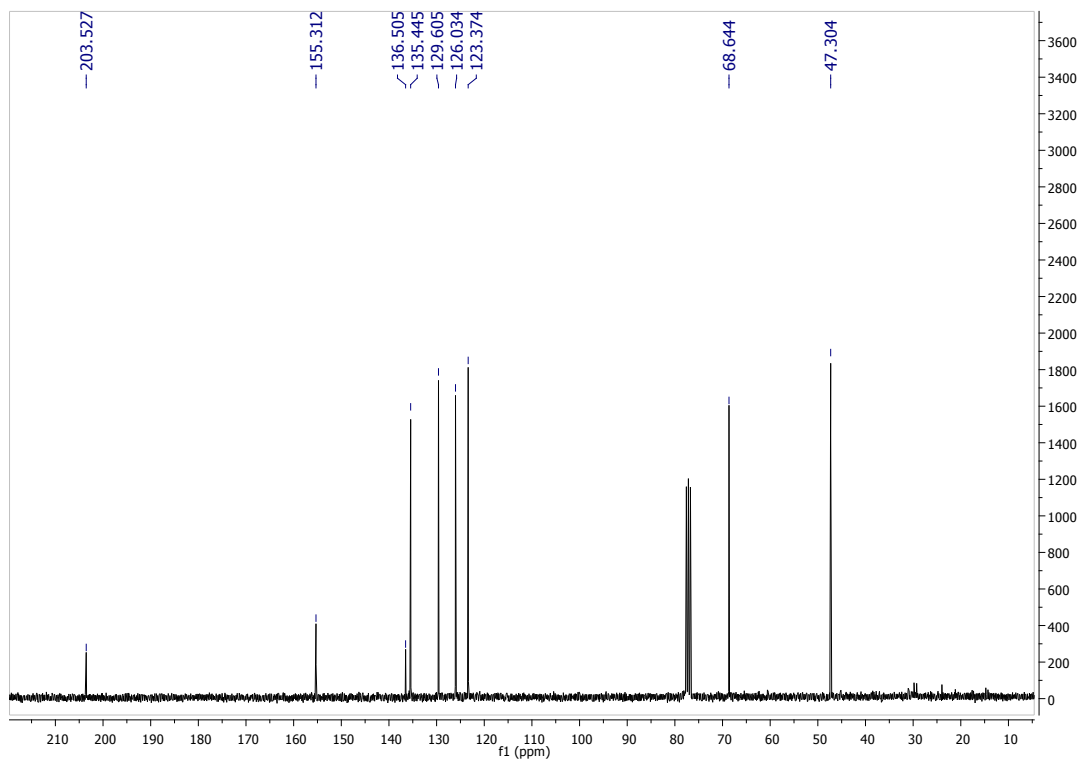
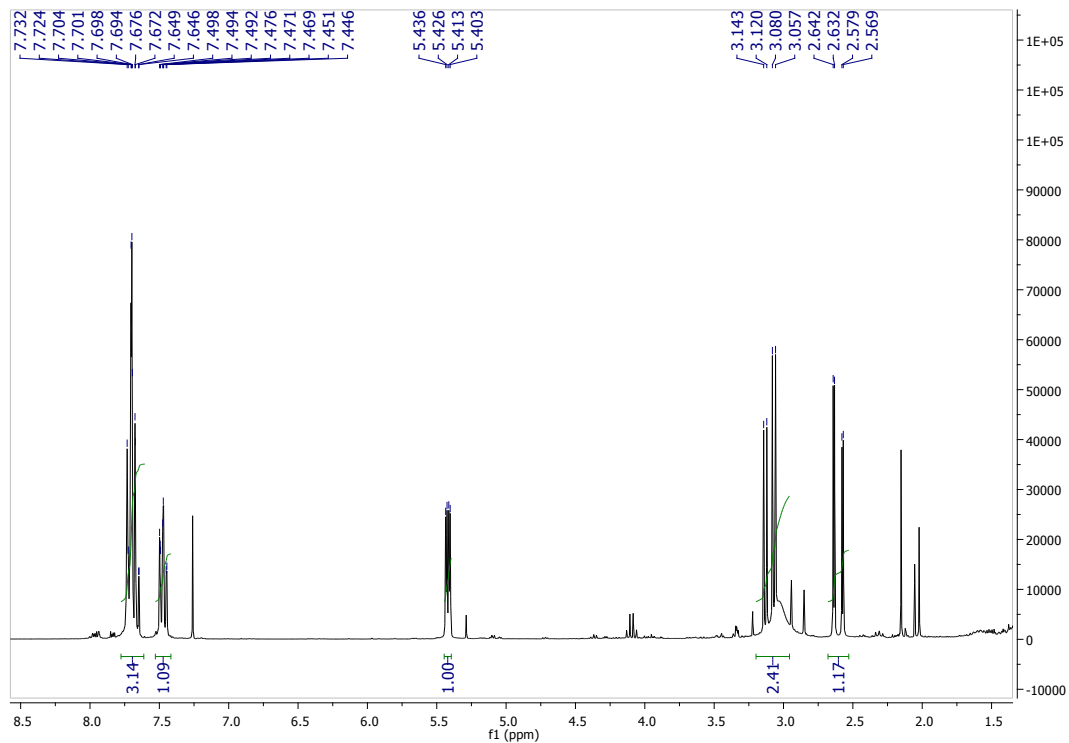
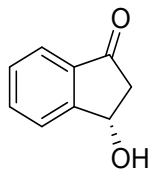
¹H NMR (300 MHz, CDCl₃) and ¹³C NMR (75 MHz, CDCl₃) spectra of 2b



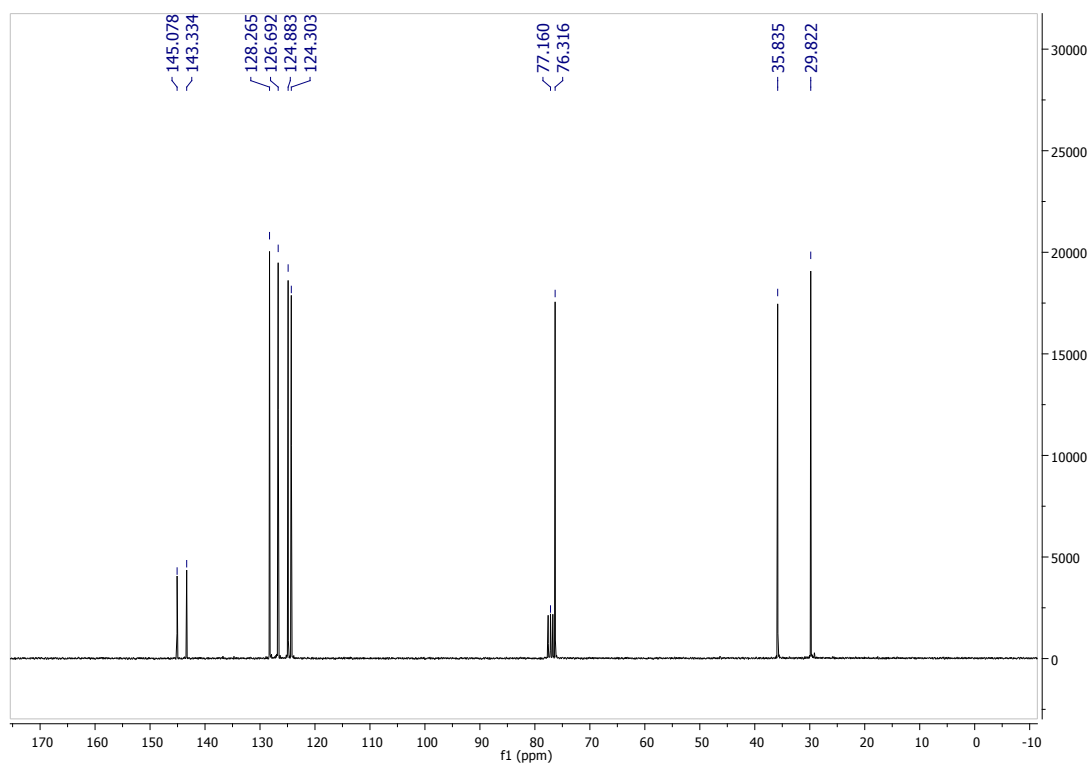
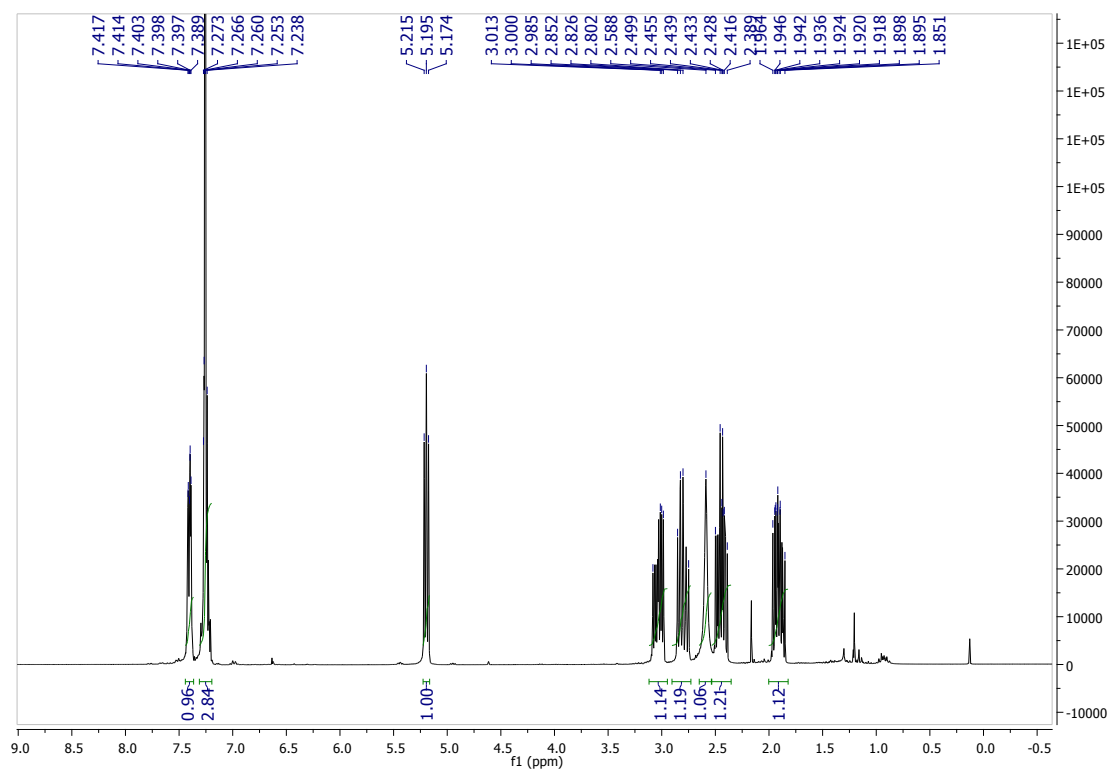
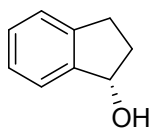
¹H NMR (300 MHz, CDCl₃) and ¹³C NMR (75 MHz, CDCl₃) spectra of 2c



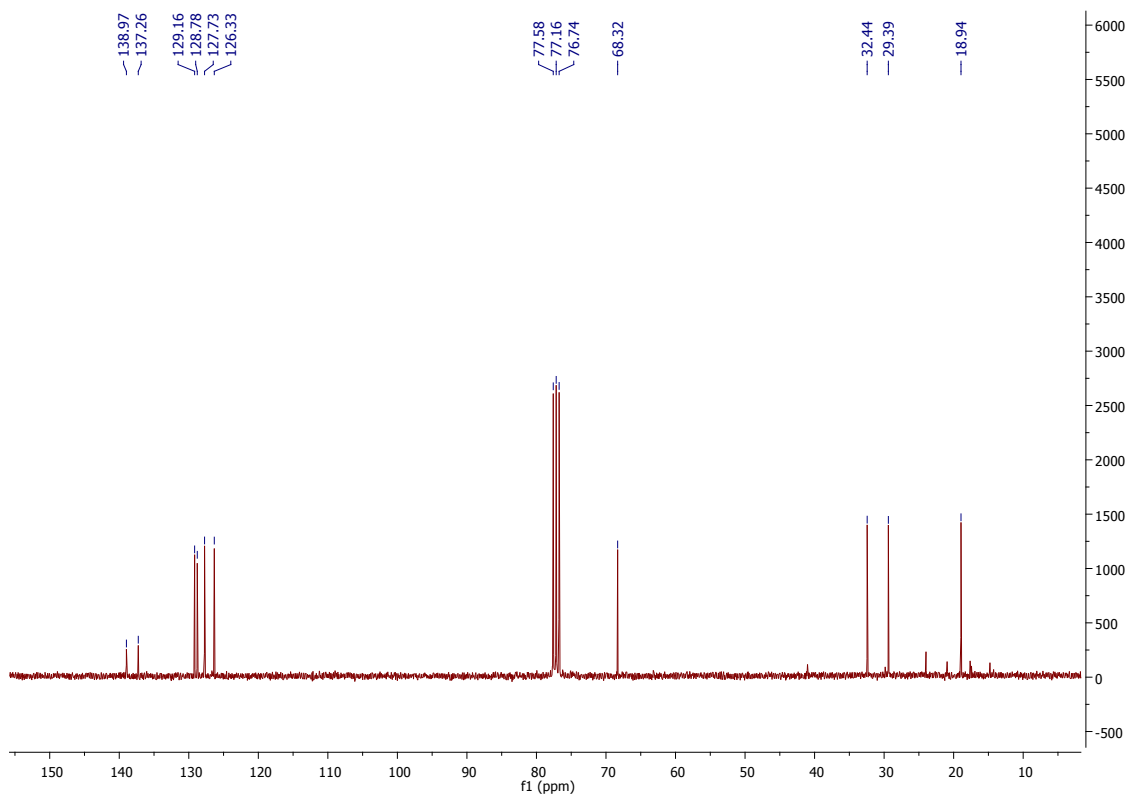
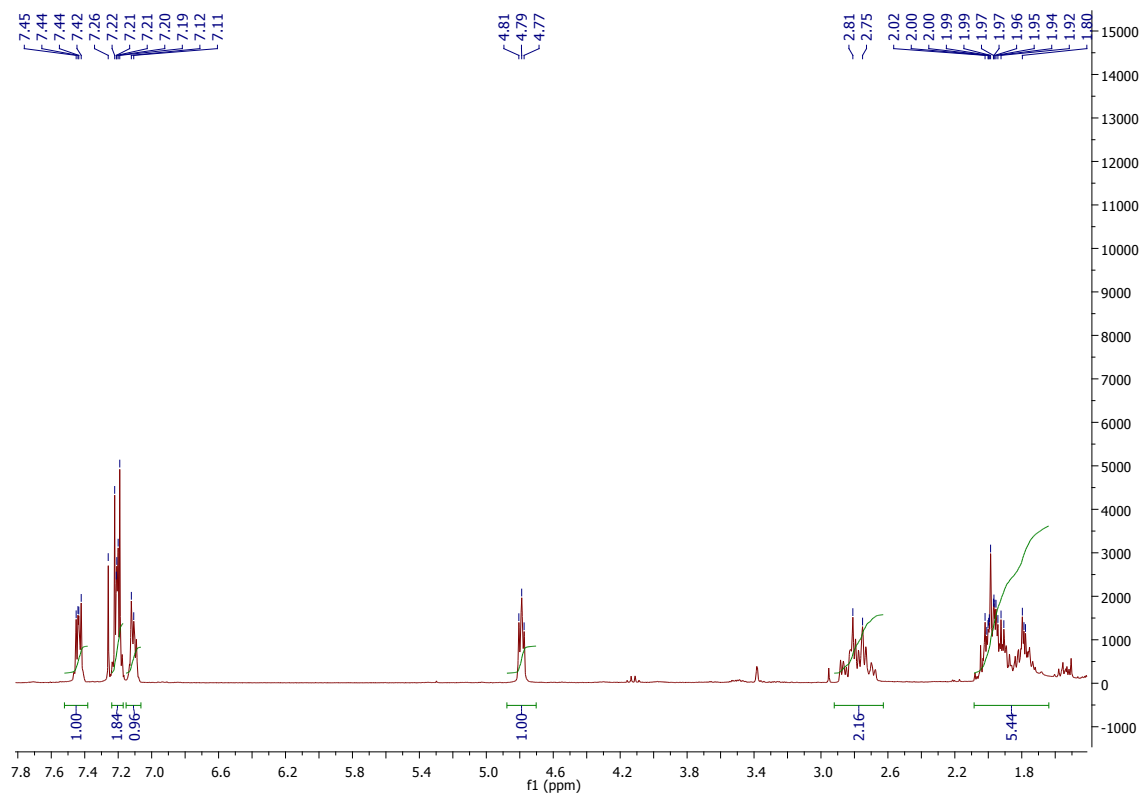
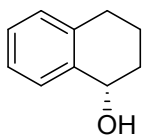
^1H NMR (300 MHz, CDCl_3) and ^{13}C NMR (75 MHz, CDCl_3) spectra of 4



¹H NMR (300 MHz, CDCl₃) and ¹³C NMR (75 MHz, CDCl₃) spectra of 6a

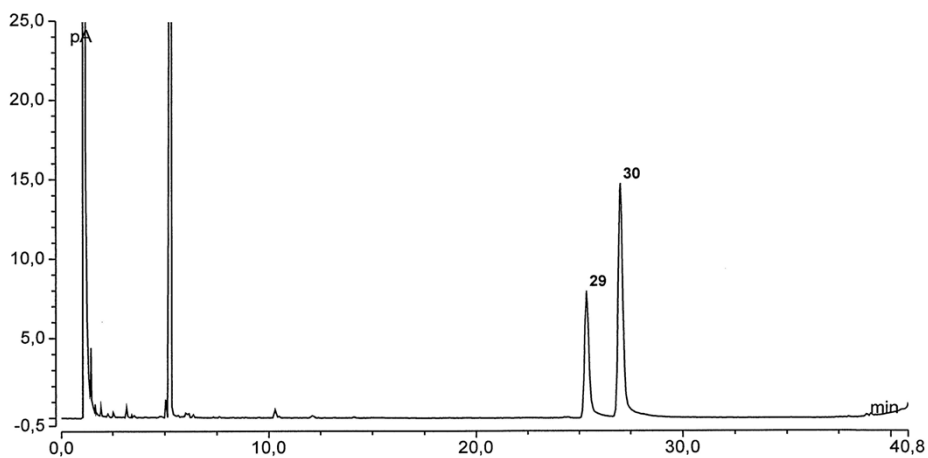


¹H NMR (300 MHz, CDCl₃) and ¹³C NMR (75 MHz, CDCl₃) spectra of 6b

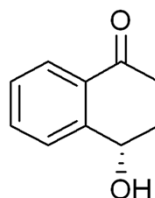


5. Selected GC chromatograms

Reaction product (2a) resulting from α -tetralone (1a) biohydroxylation reaction with WT-P450

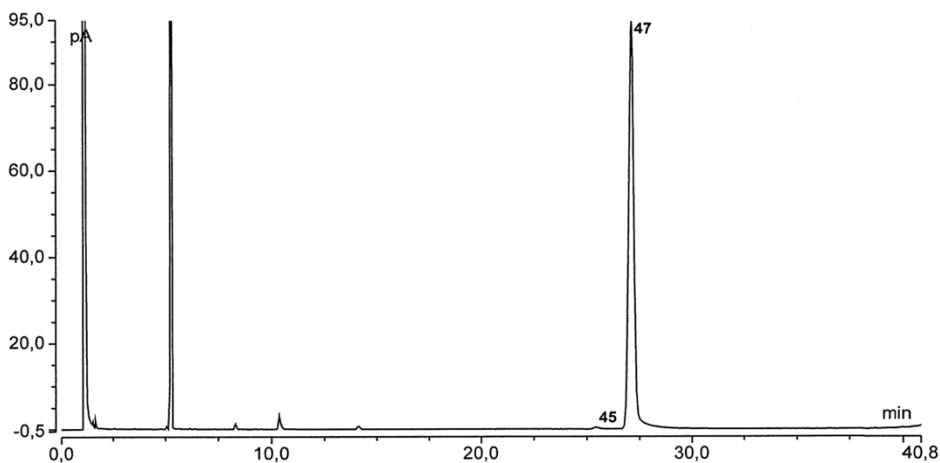


No.	Ret.Time min	Rel.Area %	Peak Name
29	25,37	33,63	(R)
30	27,02	66,37	(S)

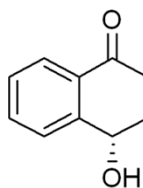


Instrument parameters:
Column: 25,0 m Hydrodex-b G/625
Temperature: 150 iso
Gas: 0,60 bar H2
Sample size: 1,0 μ L

Reaction product (2a) resulting from α -tetralone (1a) biohydroxylation reaction with A328F-P450

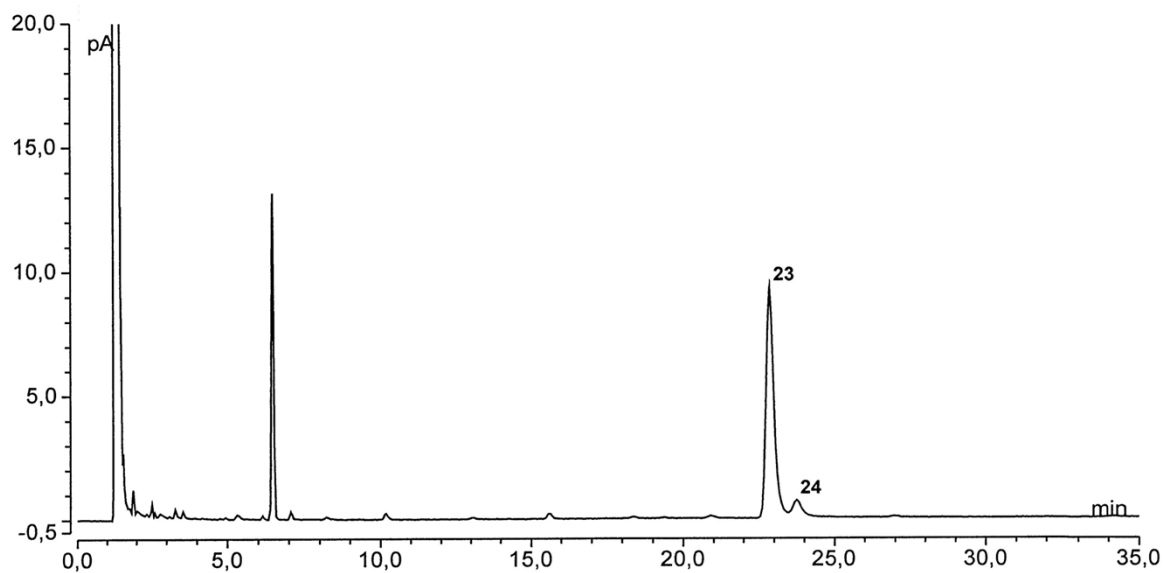
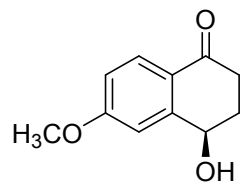


No.	Ret.Time min	Rel.Area %	Peak Name
45	25,44	0,42	(R)
47	27,16	99,58	(S)



Instrument parameters:
Column: 25,0 m Hydrodex-b G/625
Temperature: 150 iso
Gas: 0,60 bar H2
Sample size: 1,0 μ L

Reaction product (2b) resulting from 6-methoxy-3,4-dihydronaphthalen-1(2H)-one (1b) biohydroxylation reaction with WT-P450

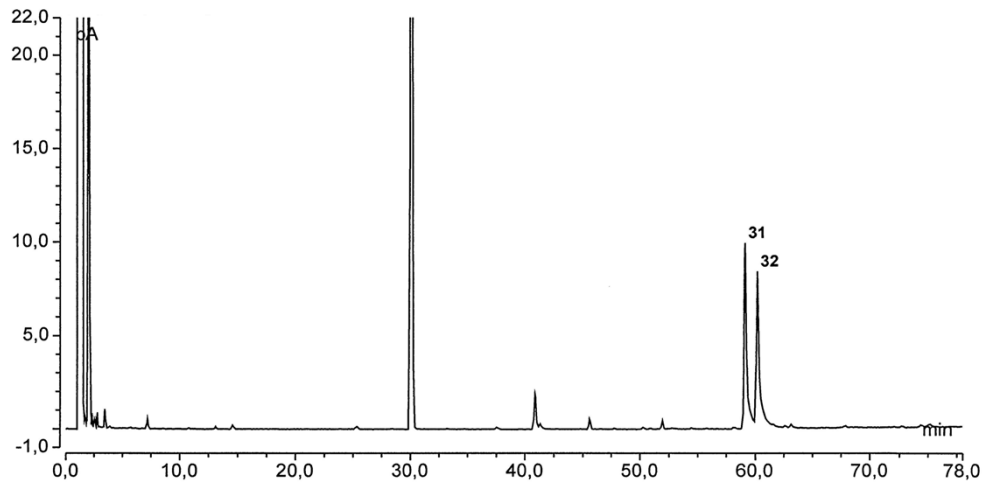
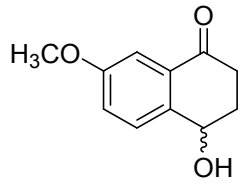


No.	Ret.Time min	Rel.Area %	Peak Name
23	22,87	91,00	
24	23,74	9,00	

Instrument parameters:

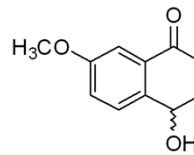
Column:	25,0 m	Hydrodex-g G/586
Temperature:	200 iso	
Gas:	0,60 bar	H2
Sample size:	1,0 µL	

Reaction product (2c) resulting from 7-methoxy-3,4-dihydronaphthalen-1(2H)-one (1c) biohydroxylation reaction with WT-P450



chirale Messung, ee-Verhältnis

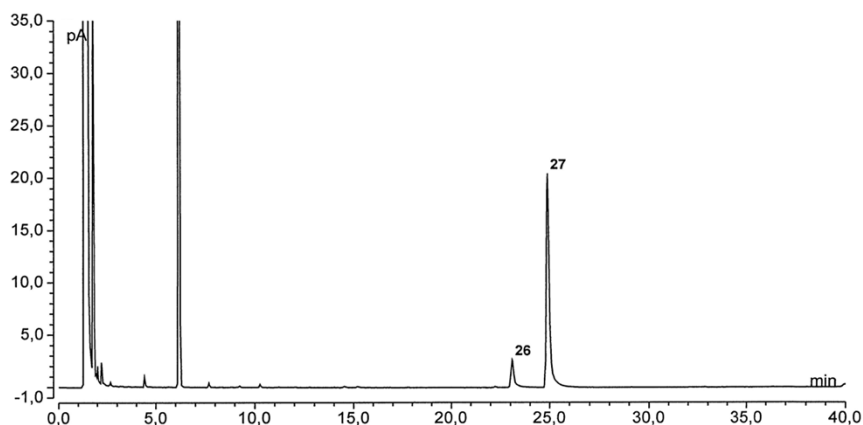
No.	Ret. Time min	Rel. Area %	Peak Name
31	59,12	49,17	
32	60,17	50,83	



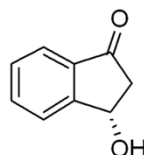
Instrument parameters:

Column:	25,0 m	Hydrodex-b G/625
Temperature:	120 1/min	
Gas:	0,60 bar	H2
Sample size:	1,0 µL	

Reaction product (4) resulting from 2,3-dihydro-1*H*-inden-1-one (3) biohydroxylation reaction with WT-P450

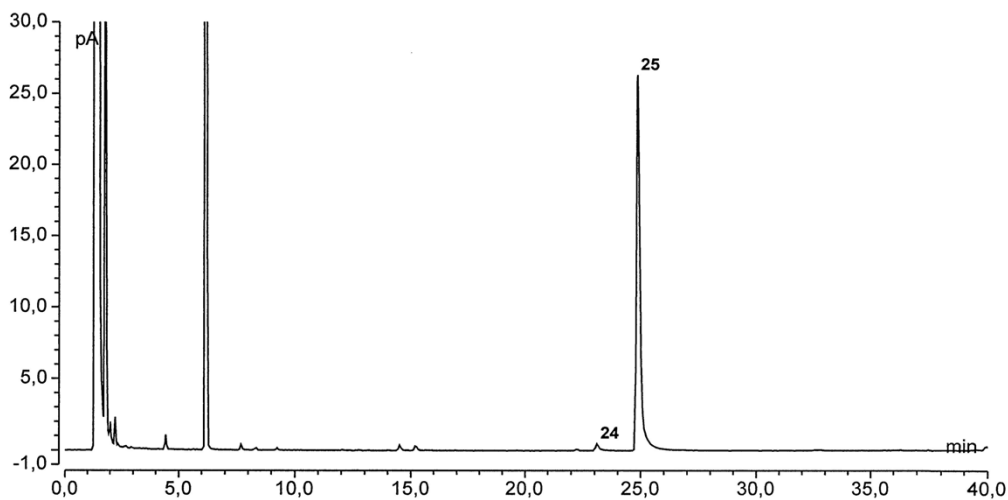


No.	Ret.Time min	Rel.Area %	Peak Name
26	23,09	12,09	(R)
27	24,89	87,91	(S)

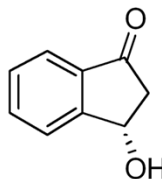


Instrument parameters:
 Column: 25,0 m Hydrodex-b G/625
 Temperature: 140 1/min 220 5min iso
 Gas: 0,50 bar H2
 Sample size: 1,0 µL

Reaction product (4) resulting from 2,3-dihydro-1*H*-inden-1-one (3) biohydroxylation reaction with A328R-P450

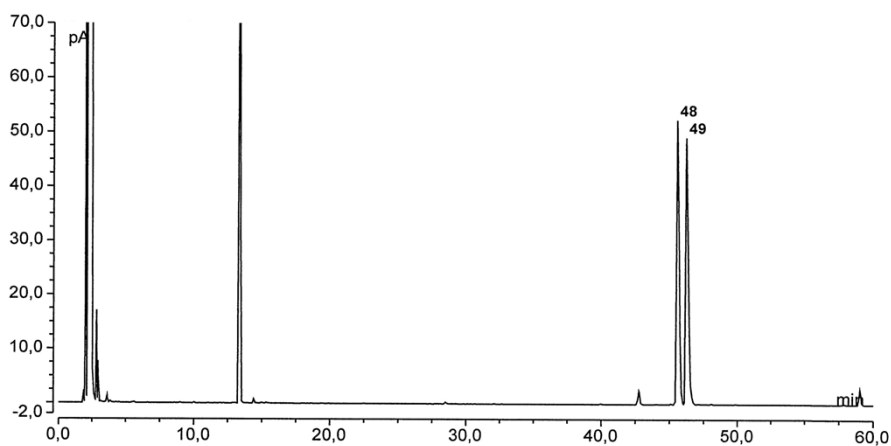


No.	Ret.Time min	Rel.Area %	Peak Name
24	23,11	2,16	(R)
25	24,87	97,84	(S)



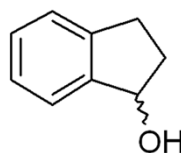
Instrument parameters:
 Column: 25,0 m Hydrodex-b G/625
 Temperature: 140 1/min 220 5min iso
 Gas: 0,50 bar H2
 Sample size: 1,0 µL

Reaction product (6a) resulting from 2,3-dihydro-1*H*-indene (5a) biohydroxylation reaction with WT-P450



chirale Messung, Racemat-Probe

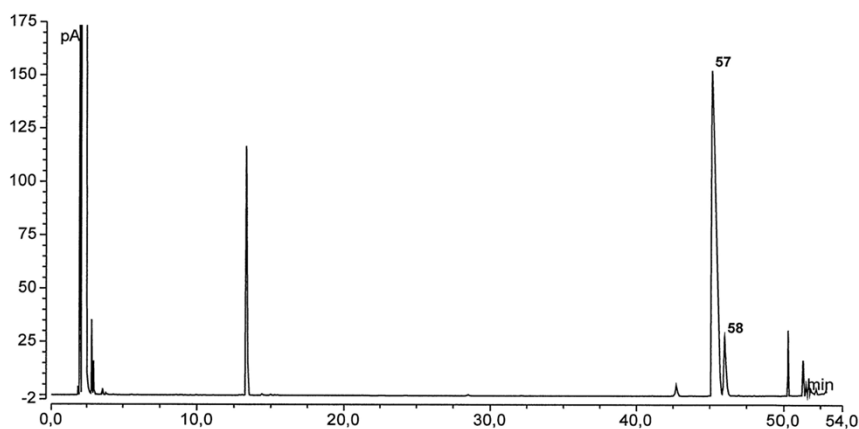
No.	Ret.Time min	Rel.Area %	Peak Name
48	45,55	50,16	
49	46,21	49,84	



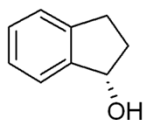
Instrument parameters:

Column: 30,0 m BGB-177/BGB-15 G/592
 Temperature: 80 1/min 220 5min iso
 Gas: 0,50 bar H2
 Sample size: 1,0 µL

Reaction product (6a) resulting from 2,3-dihydro-1*H*-indene (5a) biohydroxylation reaction with A328F-P450



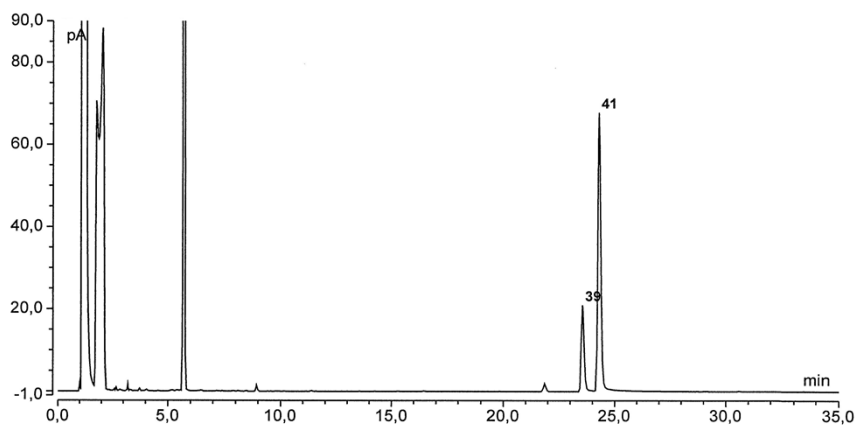
No.	Ret.Time min	Rel.Area %	Peak Name
57	45,19	91,35	(S)
58	46,03	8,65	(R)



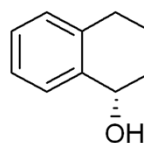
Instrument parameters:

Column: 30,0 m BGB-177/BGB-15 G/592
 Temperature: 80 1/min 125 12/min 220 5min iso
 Gas: 0,50 bar H2
 Sample size: 1,0 µL

Reaction product (6b) resulting from 1,2,3,4-tetrahydrodecaline (5b) biohydroxylation reaction with WT-P450

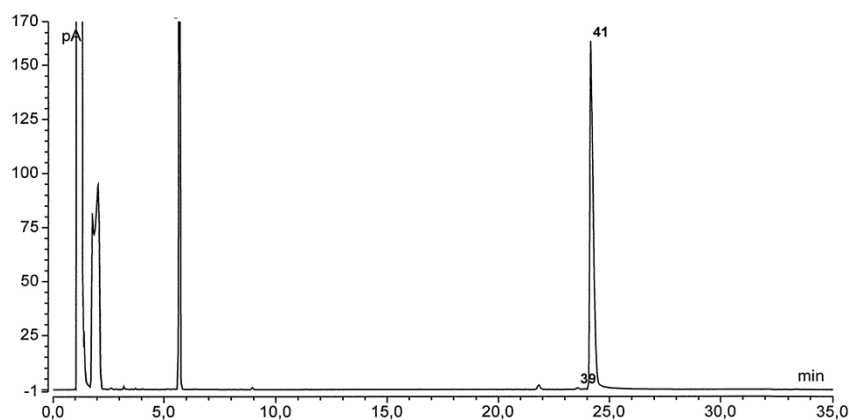


No.	Ret.Time min	Rel.Area %	Peak Name
39	23,54	21,84	(R)
41	24,28	78,16	(S)

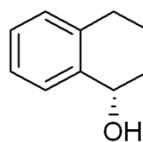


Instrument parameters:
 Column: 25,0 m Hydrodex-b G/625
 Temperature: 100 1/min 220
 Gas: 0,60 bar H2
 Sample size: 1,0 µL

Reaction product (6b) resulting from 1,2,3,4-tetrahydrodecaline (5b) biohydroxylation reaction with A328F-P450



No.	Ret.Time min	Rel.Area %	Peak Name
39	23,57	0,36	(R)
41	24,18	99,64	(S)



Instrument parameters:
 Column: 25,0 m Hydrodex-b G/625
 Temperature: 100 1/min 220
 Gas: 0,60 bar H2
 Sample size: 1,0 µL